6. Tuan RS: Cellular signaling in developmental chondrogenesis: n-cadherin, Wnts, and BMP-2. J Bone Joint Surg Am 2003, 85:137–141
7. Iwamoto M, Kitagaki J, Iwamoto M: Regulation of chondrocyte differentiation by a soluble Wnt receptor, Frzb-1. Jikken Igaku 2001, 19:1210–1214
8. Nusse R, Brown A, Papkoff J, Scambler P, Shackleford G, McMahon A, Moon R, Varmus H: A new nomenclature for int-1 and related genes: the Wnt gene family. Cell 1991, 64:231
9. Miller JR, Hocking AM, Brown JD, Moon RT: Mechanism and function of signal transduction by the Wnt/beta-catenin and Wnt/Ca2+ pathways. Oncogene 1999, 18:7860–7872
10. Seidensticker MJ, Behrens J: Biochemical interactions in the wnt pathway. Biochim Biophys Acta 2000, 1495:168–182
11. Sohn P, Crowley M, Slattery E, Serra R: Developmental and TGF-beta-mediated regulation of Ank mRNA expression in cartilage and bone. Osteoarthritis Cartilage 2002, 10:482–490
12. Moon RT, Brown JD, Torres M: WNTs modulate cell fate and behavior during vertebrate development. Trends Genet 1997, 13:157–162
13. Cadigan KM, Nusse R: Wnt signaling: a common theme in animal development. Genes Dev 1997, 11:3286–3305
14. Hsieh JC, Rattner A, Smallwood PM, Nathans J: Biochemical characterization of Wnt-frizzled interactions using a soluble, biologically active vertebrate Wnt protein. Proc Natl Acad Sci USA 1999, 96:3546–3551
15. Hartmann C, Tabin CJ: Dual roles of Wnt signaling during chondrogenesis in the chicken limb. Development 2000, 27:3141–3159
16. Sen M, Chamorro M, Reifert J, Corr M, Carson DA: Blockade of Wnt-5A/frizzled 5 signaling inhibits rheumatoid synoviocyte activation. Arthritis Rheum 2001, 44:772–781
17. Hartmann C, Tabin CJ: Wnt-14 plays a pivotal role in inducing synovial joint formation in the developing appendicular skeleton. Cell 2001, 104:341–351
18. Rudnicki JA, Brown AM: Inhibition of chondrogenesis by Wnt gene expression in vivo and in vitro. Dev Biol 1997, 185:104–118
19. Sen M, Lauterbach K, El-Gabalawy H, Firestein GS, Corr M, Carson DA: Expression and function of wingless and frizzled homologs in rheumatoid arthritis. Proc Natl Acad Sci U S A 2000, 97:2791–2796
20. Letamendia A, Labbe E, Attisano L: Transcriptional regulation by Smads: crosstalk between the TGF-beta and Wnt pathways. J Bone Joint Surg Am 2001, 83:31–39
21. Boyden LM, Mao J, Belsky J, Mitzner L, Farhi A, Mitnick MA, Wu D, Insogna K, Lifton RP: High bone density due to a mutation in LDL-receptor-related protein 5. N Engl J Med 2002, 346:1513–1521
22. Ijiri K, Nagayoshi R, Matsushita N, Tsuruga H, Taniguchi N, Gushi A, Sakakima H, Komiya S, Matsuyama T: Differential expression patterns of secreted frizzled related protein genes in synovial cells from patients with arthritis. J Rheumatol 2002, 29:2266–2270
23. Barchowsky A, Frleta D, Vincenti MP: Integration of the NF-kappaB and mitogen-activated protein kinase/AP-1 pathways at the collage-nase-1 promoter: divergence of IL-1 and TNF-dependent signal transduction in rabbit primary synovial fibroblasts. Cytokine 2000, 12:1469–1479
24. Livak KJ, Schmittgen TD: Analysis of relative gene expression data using real-time quantitative PCR and the 2(-Delta Delta C(T)) method. Methods 2001, 25:402–408
25. Shepstone L, Rogers J, Kirwan J, Silverman B: Distribution of distal femoral osteophytes in a human skeletal population. Ann Rheum Dis 2000, 59:513–520
26. Molenaar M, van de Wetering M, Oosterwegel M, Peterson Maduro J, Godsave S, Korinek V, Roose J, Destree O, Clevers H: XTcf-3 transcription factor mediates beta-catenin-induced axis formation in Xenopus embryos. Cell 1996, 9:391–399
27. Kuhl M, Sheldahl LC, Park M, Miller JR, Moon RT: The Wnt/Ca2+ pathway: a new vertebrate Wnt signaling pathway takes shape. Trends Genet 2000, 16:279–283
28. Boutros M, Paricio N, Strutt DI, Mlodzik M: Dishevelled activates JNK and discriminates between JNK pathways in planar polarity and wingless signaling. Cell 1998, 94:109–118
29. Gong Y, Slee RB, Fukai N, Rawadi G, Roman-Roman S, Reginato AM, Wang H, Cundy T, Glorieux FH, Lev D, Zacharin M, Oexle K, Marcelino J, Suwairi W, Heeger S, Sabatakos G, Apte S, Adkins WN, Allgrove J, Arslan-Kirchner M, Batch JA, Beighton P, Black GC, Boles RG, Boon LM, Borrone C, Brunner HG, Carle GF, Dallapiccola B, De Paepe A, Floege B, Halfhide ML, Hall B, Hennekam RC, Hirose T, Jans A, Juppner H, Kim CA, Keppler-Noreuil K, Kohlschuetter A, LaCombe D, Lambert M, Lemyre E, Letteboer T, Peltonen L, Ramesar RS, Romanengo M, Somer H, Steichen-Gersdorf E, Steinmann B, Sullivan B, Superti-Furga A, Swoboda W, van den Boogaard MJ, Van Hul W, Vikkula M, Votruba M, Zabel B, Garcia T, Baron R, Olsen BR, Warman ML: Osteoporosis-Pseudoglioma Syndrome Collaborative Group: LDL receptor-related protein 5 (LRP5) affects bone accrual and eye development. Cell 2001, 107:513–523
30. Saitoh T, Mine T, Katoh M: Expression and regulation of WNT8A and WNT8B mRNAs in human tumor cell lines: up-regulation of WNT8B mRNA by beta-estradiol in MCF-7 cells, and down-regulation of WNT8A and WNT8B mRNAs by retinoic acid in NT2 cells. Int J Oncol 2002, 20:999–1003
31. Hsu SC, Galceran J, Grosschedl R: Modulation of transcriptional regulation by LEF-1 in response to Wnt-1 signaling and association with beta-catenin. Mol Cell Biol 1998, 18:4807–4818
32. Hoang B, Moos M Jr, Vukicevic S, Luyten FP: Primary structure and tissue distribution of FRZB, a novel protein related to Drosophila frizzled, suggest a role in skeletal morphogenesis. J Biol Chem 1996, 271:26131–26137
33. Wang S, Krinks M, Moos M Jr: Frzb-1, an antagonist of Wnt-1 and Wnt-8, does not block signaling by Wnts -3A, -5A, or -11. Biochem Biophys Res Commun 1997, 236:502–504

Microbubble-Enhanced Ultrasound Exposure Promotes Uptake of Methotrexate Into Synovial Cells and Enhanced Antiinflammatory Effects in the Knees of Rabbits With Antigen-Induced Arthritis

Hiroyuki Nakaya,[1] Tominaga Shimizu,[2] Ken-ichi Isobe,[2] Keiji Tensho,[2] Takahiro Okabe,[2]
Yukio Nakamura,[2] Masashi Nawata,[2] Hideki Yoshikawa,[1] Kunio Takaoka,[3]
and Shigeyuki Wakitani[2]

Objective. To evaluate whether microbubble-enhanced ultrasound (US) treatment promotes the delivery of methotrexate (MTX) into synovial cells and the enhanced antiinflammatory effects of intraarticular MTX therapy in a rabbit arthritis model.

Methods. Arthritis was induced in both knees of 53 rabbits by immunization with ovalbumin. MTX including a microbubble agent was then injected into the left and right knee joints, and the right knees were exposed to US (MTX+/US+ group), while the left knees were not (MTX+/US− group). The knee joints were evaluated histologically in 7 rabbits at 5 time points up to day 56. Quantitative gene expression of interleukin-1β (IL-1β) in synovial tissue was measured on days 7 and 28. Eight rabbits were used for the measurement of MTX concentration in synovial tissue 12 hours after treatment. To evaluate the effect of microbubble-enhanced US treatment in the absence of MTX, only the microbubble agent was injected into the left and right knee joints of 10 rabbits with or without US exposure, and these animals were evaluated histologically on days 7 and 28.

Results. The MTX concentration in synovial tissue was significantly higher in the MTX+/US+ group than in the MTX+/US− group. Synovial inflammation was less prominent in the MTX+/US+ group compared with the MTX+/US− group, judging from the results of the histologic evaluation and the gene expression levels of IL-1β in synovial tissue. It also appeared that microbubble-enhanced US exposure itself did not affect inflammation.

Conclusion. Microbubble-enhanced US exposure promoted the uptake of MTX into synovial cells, which resulted in enhancement of the antiinflammatory effects of the intraarticular MTX injection. These results suggest that application of this technique may have clinical benefit.

Rheumatoid arthritis (RA) is a systemic inflammatory disorder characterized by pain, swelling, and destruction of the affected joints. The exact mechanism of RA pathogenesis is not well understood. Recently, remarkable progress in the area of anticytokine therapy has provided an alternative and successful approach for therapeutic intervention in RA. However, methotrexate (MTX) still plays a central role in the treatment of RA, although administration of this agent sometimes causes serious side effects, such as interstitial pneumonia, renal failure, and myelosuppression. Intraarticular injection of MTX is thought to be safe compared with the systemic administration of this agent, although the clinical effectiveness in controlling synovitis in RA patients is controversial. Most studies have documented insufficient antiinflammatory effects (1–3). Mechanisms of resis-

tance to MTX are considered to consist of 3 parts: decreased transport, impaired polyglutamylation, and increased dihydrofolate reductase enzyme activity (4–6). It has been reported that there is a significant correlation between reduced levels of folate carrier protein (one of the MTX transporters) at diagnosis and the histologic responses to preoperative MTX chemotherapy for osteosarcoma (6). From these observations, it is possible to conclude that the efficacy of MTX is limited by its transport into cells. Thus, we hypothesized that poor delivery of MTX into RA synovial cells would lead to poor clinical efficacy of intraarticular MTX injection therapy.

To facilitate uptake of MTX into synovial cells, we chose an ultrasound (US) treatment technique (sonoporation) with enhancement by the use of an echo-contrast microbubble agent. Previous reports have indicated that US exposure increases transfection efficiency of gene constructs, due to increased cell membrane porosity and acoustic cavitation (7,8), which is enhanced with the use of microbubble agents. This is one of the best techniques for in vivo work and clinical applications because it is simple and noninvasive. Additionally, there are no viral components, although the success rate for induction is lower than that found with viral technologies in vitro and in vivo, as previously reported (9–12). Our findings in the present study indicate that US irradiation treatment with a microbubble agent enhances the antiinflammatory effect of intraarticular MTX injection in an ovalbumin (OVA)–induced arthritis model in rabbits.

MATERIALS AND METHODS

In vitro induction of fluorescence-conjugated MTX. As an initial step, we determined the optimum concentration of echo-contrast microbubbles (Optison; Mallinckrodt, St. Louis, MO) for MTX (Iatron, Tokyo, Japan) induction into synovial cells. In vitro induction was performed according to a previously described procedure (10). Synovial cells were obtained during total knee arthroplasty from 2 RA patients, who had provided informed consent. Briefly, the tissue was minced and incubated with 0.25% collagenase (Roche, Indianapolis, IN) in phosphate buffered saline (PBS) for 2 hours at 37°C under continuous agitation. The cells were collected by centrifugation, resuspended, and cultured in Dulbecco's modified Eagle's medium (Invitrogen, Carlsbad, CA) containing 10% fetal calf serum and antibiotics (100 units/ml penicillin, 0.1 mg/ml streptomycin, 0.25 μg/ml amphotericin B; Invitrogen). Cultured cells were trypsinized, washed twice in PBS, and resuspended at 1×10^5/ml of PBS per well in a 48-well plate. Optison was added to the cell medium at concentrations of 0%, 5%, 10%, and 20%. Then, 10 μg of Texas Red–conjugated

MTX (Molecular Probes, Leiden, The Netherlands) was added to the cell supernatant in each well.

The US probe and well plate were firmly fixed to a stand to avoid dislocation during US exposure. Immediately after fluorescent MTX and microbubbles were added to the well, US exposure was performed. The sonoporator (Sonitron 2000; Mallinckrodt) settings were as follows: frequency 1 MHz, duration 30 seconds, power 1.0 W/cm², duty cycle 10%, and probe diameter 0.5 cm. The US probe was inserted directly into the cell suspension. A miniature stirrer was placed within the well and spun at 300 revolutions per minute to prevent cell adhesion to the plate. The cells were placed a row apart from each other to prevent interaction due to the transmission of US between the wells. After US exposure, cell viability was tested by counting the cells stained with trypan blue. The cell suspensions were harvested from the wells and attached to slides using a Cyto-Tek centrifuge (Sakura, Tokyo, Japan) at 1,500 rpm for 5 minutes. Texas Red–positive cells were detected by fluorescence microscopy. The average induction efficiency was calculated as the ratio of incorporated cells to all cells in 5 fields.

In vivo induction of fluorescence-conjugated MTX. To confirm that MTX induction into synovial in vivo cells would be promoted by microbubble-enhanced US treatment, we designed in vivo experiments. Three NZW rabbits (Japan SLC, Hamamatsu, Japan) weighing 2.5, 2.7, and 2.8 kg were anesthetized by intramuscular injection of a mixture of ketamine (100 mg/ml [0.6 ml/kg body weight]; Sankyo, Tokyo, Japan) and xylazine (20 mg/ml [0.3 ml/kg body weight]; Bayer, Leverkusen, Germany). We injected 50 μg of Texas Red–conjugated MTX with 5% Optison in 2.5 ml saline, making sure to diffuse it into the left and right knee joints. Soon after injection, US exposure was applied in the medial, central, and lateral areas of the suprapatellar pouch of the right knees for 2 minutes per application. US treatment was not performed in the left knees. US was administered with a sonoporator using the following settings: frequency 1 MHz, duration 2 minutes, power 2.0 W/cm², duty cycle 50%, and probe diameter 3 cm. Then, the rabbits were killed by excessive intravenous injection of anesthetic agents. Synovial tissue, with the associated muscle and tendon of the suprapatellar pouch of the joints, was obtained and dissected sagittally at the center. It was immediately chilled in liquid nitrogen. Sections of 7-μm thickness were cut in a cryostat, air-dried on slides, fixed in 4% paraformaldehyde, and stained with hematoxylin for counterstaining. The sections were examined by fluorescence microscopy.

Antigen-induced arthritis (AIA) in the rabbit knee. Sixty-two NZW rabbits, each weighing ~2.7 kg (2.5–3.1 kg) were anesthetized as described above. They then received intradermal injections of 4 mg OVA (Sigma, St. Louis, MO) in 0.5 ml Freund's complete adjuvant (Difco, Detroit, MI) and 0.5 ml PBS 3 times at 7-day intervals, as previously reported (13). Five days after the third injection, 1.5 mg OVA in 0.5 ml sterile saline was injected into the left and right knee joints of the rabbits. After confirming the establishment of arthritis 10 days after the injection, the experimental procedures were started. Fifty-three of the 62 rabbits (85%) showed signs of arthritis in both knees and were used for the experiments. In preliminary experiments, we confirmed that the inflammation was virtually identical histologically in both knees (data not shown).

MTX injection and US treatment. We injected 0.1% MTX with 5% Optison (from the initial in vitro experiment described above) in 2.5 ml saline, ensuring diffusion into both knee joints of 43 rabbits that were anesthetized as described above. US was administered to the right knee in the same manner (MTX+/US+ group). US treatment was not performed on the left knees (MTX+/US− group). Seven rabbits each were killed on days 3, 7, 14, 28, and 56 for histologic examination. The remaining 8 rabbits were used for measurement of MTX in synovial tissue.

To determine whether microbubble-enhanced US itself affected inflammation of synovial tissue, we injected 5% Optison without MTX in 2.5 ml saline into the left and right knee joints of the other 10 rabbits. Then, US was administered to the right knees (MTX−/US+ group) in the same manner as described above, while the left knees were not exposed (MTX−/US− group). Five rabbits each were killed on days 7 and 28 for histologic evaluation.

Histologic evaluation. Synovial tissue from the suprapatellar pouch of the joints was obtained at each time point. It was dissected sagittally at the center, washed, and fixed in 10% formaldehyde in PBS. It was then rinsed with deionized water and dehydrated in a graded ethanol series. Dehydrated tissue was embedded in paraffin, cut into 5-μm sections, mounted on glass slides precoated with poly-L-lysine, dried overnight at 50°C, and stained with hematoxylin and eosin (H&E).

Distal femurs were cut sagittally in the center of the patellar groove and fixed in 10% formaldehyde, decalcified in 10% EDTA, embedded in paraffin, cut into 5-μm sections, and stained with H&E and toluidine blue.

To evaluate the degree of synovial inflammation, we used modified scoring criteria as previously described by Sanchez-Pernaute and colleagues (14). These criteria (Table 1) consist of 5 categories: inflammatory cell infiltration, synovial lining layers, villus formation, vascularity, and cartilage damage. Synovial tissue was scored depending on the degree of inflammation (from 0 for normal tissue to 18 for most severe inflammation). Sections were examined blindly and scored independently by 3 of the authors (KT, TO, YN), without knowledge of the group being examined.

Immunohistochemistry. To identify blood vessels accurately, anti–α-smooth muscle actin (α-SMA) immunostaining was performed using the mouse monoclonal anti–α-SMA antibody (1A4; Dako, Carpinteria, CA) and the Envision Plus HRP system (K4006; Dako). Formalin-fixed paraffinized sections of rabbit synovial tissue were baked, dewaxed, and rehydrated prior to a peroxidase block (0.1% [volume/volume] H_2O_2). The primary antibody and the horseradish peroxide–labeled polymer were used as per the Dako Envision kit, followed by staining with 3,3′-diaminobenzidine and counterstaining with hematoxylin before mounting. A negative control was prepared by omitting the primary antibody. A positive control was prepared on the vessels of the same section.

Measurement of MTX concentrations. MTX and Optison in 2.5 ml saline were injected into the left and right knee joints of 8 rabbits. US was administered to the right knees in the same manner, while the left knees were not exposed to US. The concentration of MTX in the synovial tissue of 8 rabbits was measured by the enzyme immunoassay method with an MTX assay kit (Iatron) 12 hours after US irradiation. Briefly,

Table 1. Scoring system for histologic evaluation

Parameter	Scoring
Inflammation	0 = normal
	1 = minimal inflammatory infiltration
	2 = mild inflammatory infiltration
	3 = moderate inflammatory infiltration
	4 = marked infiltration with marked edema
	5 = severe infiltration with edema
Synovial lining layers	0 = normal (1–2 cell layers)
	1 = slightly hyperplasia (2–3 cell layers)
	2 = moderate (3–5 cell layers)
	3 = pronounced (5 or more cell layers)
Villus formation	0 = none
	1 = minimal (1–2 villi)
	2 = several (3 or more villi)
Vascularity	0 = normal (limited number of blood vessels)
	1 = slightly hypervascular (focal occurrence of a small number of blood vessels)
	2 = moderate (focal occurrence of a large number of blood vessels)
	3 = pronounced (broadly distributed and large number of blood vessels)
Cartilage damage	0 = normal
	1 = minimal (loss of toluidine blue staining only)
	2 = mild (loss of toluidine blue staining and mild cartilage thinning)
	3 = moderate (moderate diffuse or multifocal cartilage loss)
	4 = marked (marked diffuse or multifocal cartilage loss)
	5 = severe (diffuse or multifocal cartilage loss)

the synovial tissue excised from the surface of inflamed synovium was homogenized in Tris buffer (pH 7.4; 3 ml/gm tissue), boiled for 5 minutes, and then centrifuged at 30,000 rpm for 30 minutes in a 4°C atmosphere. This was followed by the addition of 0.1 ml of the supernatant in 1 ml of reagent composed of dihydrofolate reductase (enzyme), NADPH (coenzyme), and 0.1 ml of dihydrofolate (substrate). The residual activity of the dihydrofolate reductase was assayed by absorptiometry at a wavelength of 340 nm.

Real-time polymerase chain reaction (PCR). Synovial tissue was obtained and messenger RNA (mRNA) expression was assessed quantitatively in 7- and 28-day samples of the MTX+/US+ and MTX+/US− groups. PCR primers and fluorogenic probes of interleukin-1β (IL-1β) (forward 5′-TTGCTGAGCCAGCCTCTCTT-3′, reverse 5′-GCTGGG-TACCAAGGTTCTTTGA-3′, TaqMan 5′-TGCCATTCAG-GCAAGGCCAGC-3′) were designed according to the published sequences (GenBank accession no. M_26295) using Primer Express software (Perkin-Elmer Applied Biosystems, Foster City, CA). They were obtained purified by high-performance liquid chromatography from Applied Biosystems. The fluorogenic probes contained a reporter dye (FAM) covalently linked at the 5′ end and a quencher dye (TAMRA) covalently attached at the 3′ end. Extension from the 3′ end was blocked by the attachment of a 3′-phosphate group.

As external controls for the target gene, plasmid recombinants containing the specific target sequence were

generated, as well as 18S ribosomal RNA (rRNA; Perkin-Elmer Applied Biosystems). For this purpose, total RNA from individuals positive for the allele of interest was extracted and reverse transcribed as described above. Following reverse transcription and allele-specific PCR, amplicons were cloned using pCR 2.1 TOPO (Invitrogen). Recombinant plasmids were expressed in competent *Escherichia coli* (INVαF'; Invitrogen). Plasmid DNA was isolated using silica cartridges (QIAprep Spin Miniprep Kit; Qiagen, Hilden, Germany). Sequences of the cloned amplicons were verified using an automated sequencer (ABI PRISM 7700; Perkin-Elmer Applied Biosystems) with universal M13 primers. Concentrations of the recombinant plasmids were determined by optical density spectrometry. Serial dilutions from the resulting clones were used for standardization, as described in detail in the manufacturer's bulletin.

PCR was performed using 300 nM forward and reverse primers and 200 nM TaqMan probe (final concentration). Each PCR amplification was performed in triplicate wells using the following temperature and cycling profile: 50°C for 2 minutes and 95°C for 10 minutes, followed by 40 cycles of 95°C for 15 seconds and 58°C for 1 minute (15).

The relative expression of IL-1β alleles was determined with reference to the total amount of IL-1β mRNA after normalization against 18S rRNA as implemented in the ABI PRISM 7700 Sequence Detection System software. Results were considered only if the analysis of IL-1β showed all reactions to have the same amount of amplification as 18S rRNA. This procedure allowed for comparison of group-specific IL-1β expression as well as the total expression levels of 18S rRNA.

Statistical analysis. Results are expressed as the mean ± SD. The significance of the difference in histologic scores between the MTX+/US+ and MTX+/US− groups at the various posttreatment times (days 3, 7, 14, 28, and 56) was tested using two-way factorial analysis of variance (ANOVA), followed by Student's paired t-test for comparison.

The difference in histologic scores among the MTX+/US+ group and the other 3 control groups (MTX+/US−, MTX−/US+, and MTX−/US−) at 7 and 28 days was compared by Student's paired t-test. Student's paired t-test was also used to analyze the results of MTX concentration and real-time reverse transcriptase–PCR. P values less than 0.05 were considered significant.

RESULTS

In vitro MTX induction into synovial cells. To confirm the promotion of MTX induction into RA synovial cells by US irradiation and to determine the optimum concentration of Optison, fluorescence-conjugated MTX was administered into RA synovial cells by sonoporation in vitro. In the absence of US, MTX was administered into a few synovial cells. With US exposure, the administration rate was increased to almost 5% for MTX alone, and ~31% with 5% Optison (Figure 1). Further increases in the concentration of this reagent elevated the induction rate to a maximum of
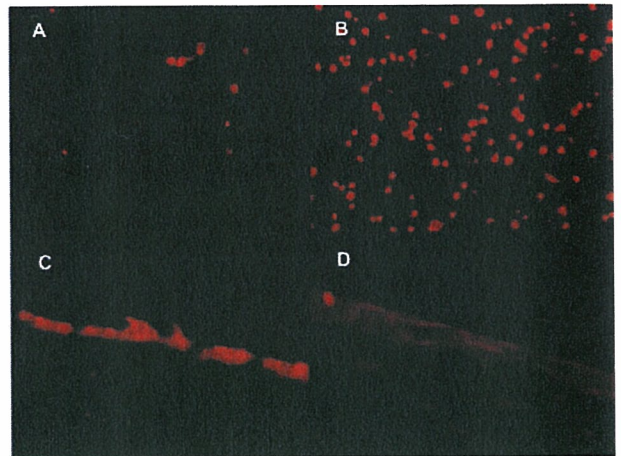

Figure 1. Fluorescence photomicrographs of synovial cells and tissue treated with Texas Red–conjugated methotrexate (MTX). Texas Red–conjugated MTX was administered to rheumatoid arthritis (RA) synovial cells by sonoporation in vitro alone (**A**) or with 5% Optison (**B**). Synovial tissue was collected from joints after injection of Texas Red–conjugated MTX with 5% Optison, with (**C**) or without (**D**) ultrasound (US) treatment. The upper parts of **C** and **D** show the joint cavity. Without Optison, almost 5% of cells were fluorescence positive (**A**). The ratio of fluorescence-positive cells was elevated to ~31% with the addition of 5% Optison (**B**). In several layers of the synovial lining, with US treatment, fluorescence-positive cells were observed (**C**). Without US, only a weakly positive area was observed (**D**). (Original magnification × 200.)

48%. For the studies described here, 5% Optison was used in each of the experiments.

In vivo MTX induction into synovial cells. To confirm the promotion of MTX induction in vivo into RA synovial cells by US treatment, fluorescence-conjugated MTX was administered into RA synovial cells by sonoporation in vivo. In the presence of US, fluorescence-positive cells were observed in several synovial lining layers, while only a weakly positive area was observed in the absence of US (Figure 1). The Texas Red–positive area was restricted to synovial cells, and was not observed in other tissue such as tendon or muscle in either group.

MTX concentration. The MTX concentrations in synovial tissue were measured in the MTX+/US+ and MTX+/US− groups (8 samples each) 12 hours after the injection of MTX and Optison. The mean ± SD weight of the tissue from right knees (the MTX+/US+ group) was 454 ± 37.0 mg, while that from left knees (the MTX+/US− group) was 467 ± 44.4 mg. There was no significant difference between these groups. The mean ± SD MTX concentration in the MTX+/US+ group was estimated at 7.575 ± 1.590 × 10^{-7} mg/dl,
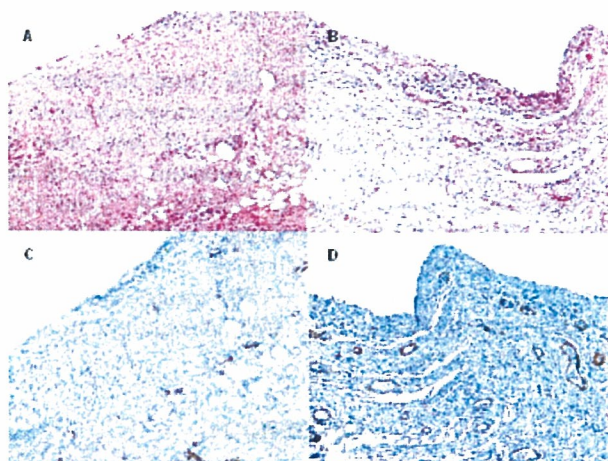
Figure 2. Day-7 histologic images of synovial tissue in the MTX+/US+ group and the MTX+/US− group. **A** and **B,** Hematoxylin and eosin staining. **C** and **D,** Immunohistochemical staining with anti–α-smooth muscle actin antibody. **A** and **C,** In the MTX+/US+ group (histologic score 3), minimal inflammatory cell infiltration, several synovial lining layers, no villus formation, and slight hypervascularity were observed. **B** and **D,** In the MTX+/US− group (histologic score 9), marked inflammatory cell infiltration, proliferating synovial lining layers (as many as 5 layers), no villus formation, and general occurrence of a large number of blood vessels were seen. See Figure 1 for definitions. (Original magnification × 40.)

while that in the MTX+/US− group was 2.875 ± 0.7889 × 10^{-7} mg/dl ($P < 0.01$).

Histologic findings. In the MTX+/US+ group, moderate inflammation (inflammatory cell infiltration, thickened synovial lining layers, and hypervascularity) was observed after 3 days, but it became less severe over a period from 7 to 56 days. Evidence of inflammation decreased in the synovial lining layer and the vascular network. In the MTX+/US− group, moderate inflammation similar to that seen in the MTX+/US+ group was observed after 3 days, continued until 28 days, and became less severe after 56 days.

After 7 days (Figure 2), in the MTX+/US+ group, minimal inflammatory cell infiltration and slight hypervascularity (minimal inflammation) were observed. In the MTX+/US− group, marked inflammatory cell infiltration, proliferating synovial lining layers (as many as 5), and proliferating blood vessels (moderate inflammation) were observed.

After 28 days (Figure 3), in the MTX+/US+ group, moderately proliferating synovial lining layers and focal proliferation of a small number of blood vessels (minimal inflammation) were observed. In the MTX+/US− group, marked inflammatory cell infiltra-

tion, proliferating synovial lining layers (>5 cell layers), and general proliferation of blood vessels (moderate inflammation) were observed.

After 56 days, both groups showed moderately proliferating synovial lining layers and focal proliferation of a small number of blood vessels (minimal inflammation). There was no significant difference between the 2 groups.

Articular cartilage was examined histologically for signs of damage caused by US exposure and/or MTX injection. A very slight decrease in the intensity of metachromatic staining (histologic scoring 0 or 1) in the surface area was observed in some samples of the MTX+/US+ and MTX+/US− groups on days 7 and 28.

Histologic scores. The mean ± SD histologic scores at 3, 7, 14, 28, and 56 days after treatment were 9.00 ± 0.31, 5.42 ± 0.30, 4.71 ± 0.18, 4.57 ± 0.37, and 5.57 ± 0.30, respectively, in the MTX+/US+ group, and 8.42 ± 0.20, 8.57 ± 0.37, 8.43 ± 0.20, 8.29 ± 0.36, and 5.71 ± 0.29 in the MTX+/US− group. The scores in the MTX+/US+ group and the MTX+/US− group were significantly different by two-way factorial ANOVA ($P < 0.05$). In addition, when we compared them at each
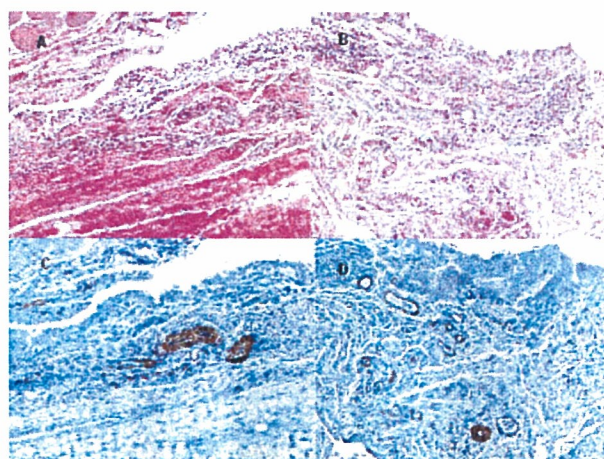

Figure 3. Day-28 histologic images of synovial tissue in the MTX+/US+ group and the MTX+/US− group. **A** and **B,** Hematoxylin and eosin staining. **C** and **D,** Immunohistochemical staining with anti–α-smooth muscle actin antibody. **A** and **C,** In the MTX+/US+ group (histologic score 5), minimal inflammatory cell infiltration, a moderate number of synovial lining layers, no villus formation, and focal occurrence of a small number of blood vessels were seen. **B** and **D,** In the MTX+/US− group (histologic score 10), marked inflammatory cell infiltration with marked edema, >5 pronounced synovial lining layers, no villus formation, and a broadly distributed large number of blood vessels were seen. See Figure 1 for definitions. (Original magnification × 40.)
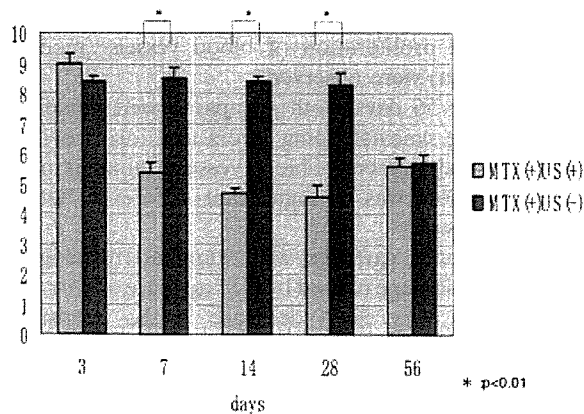
Figure 4. Histologic scores of synovial tissue from patients in the MTX+/US+ and MTX+/US− groups at each time point. Values are the mean and SD. *P* values were determined using two-way factorial analysis of variance. See Figure 1 for definitions.

time point using Student's paired *t*-test, the scores in the MTX+/US+ group at 7, 14, and 28 days were significantly better than those in the MTX+/US− group (Figure 4).

To confirm that the antiinflammatory effect was not due to US exposure, we injected the right knees with Optison only and exposed them to US (MTX−/US+ group). Scores in the MTX+/US+, MTX+/US−, MTX−/US+, and MTX−/US− groups were compared on days 7 and 28, and a significant difference was
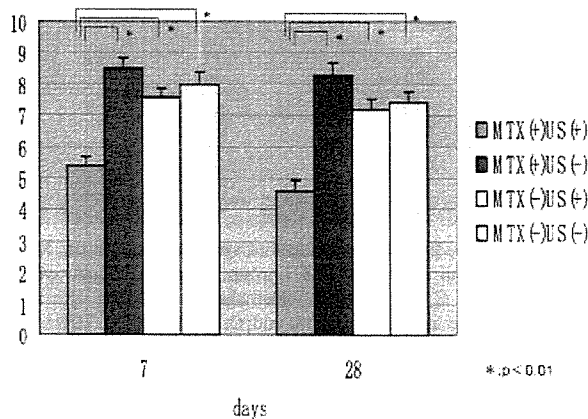
Figure 5. Histologic scores of synovial tissue from patients in the MTX+/US+, MTX+/US−, MTX−/US+, and MTX−/US− groups 7 and 28 days after treatment. Values are the mean and SD. See Figure 1 for definitions.

observed between the MTX+/US+ group and the other 3 groups (*P* < 0.05) (Figure 5).

Findings of real-time PCR. Using real-time PCR, we examined the quantitative gene expression of IL-1β in synovial tissue obtained 7 and 28 days after US irradiation. The mean ± SD expression 7 and 28 days after treatment was 1.3×10^{-3} (1.5×10^{-4}) and 3.3×10^{-3} (2.5×10^{-4}), respectively, in the MTX+/US+ group, and 8.6×10^{-2} (9.0×10^{-3}) and 8.4×10^{-2} (1.2×10^{-3}) in the MTX+/US− group. There was a significant difference (*P* < 0.01) between the groups at each time point.

DISCUSSION

Our results show that, in a rabbit arthritis model, microbubble-enhanced US treatment promotes uptake of MTX into synovial cells, which results in acceleration of antiinflammatory effects following intraarticular MTX injection. The antiinflammatory effect was confirmed by histologic scoring and expression of IL-1β mRNA in synovial tissue. The increased uptake of MTX into synovial cells was confirmed histologically by analysis of MTX concentration in synovial tissue and induction of Texas Red–conjugated MTX in vitro and in vivo. To confirm that the antiinflammatory effect was not due to US irradiation treatment with or without Optison, we injected Optison only (without MTX), and administered US to the right knees in the rabbits. Because there was no antiinflammatory effect, we concluded that neither microbubble injection with US exposure nor MTX injection has an antiinflammatory effect. However, the combination of MTX, microbubble injection, and US exposure was very effective. To our knowledge, this is the first report to describe the use of US in conjunction with antiinflammatory joint therapy in vivo. US gained attention through its use in gene therapy and tissue engineering. It is safe, minimally invasive, and can accommodate different therapeutic applications.

An antiinflammatory effect of this procedure (significantly reduced histologic inflammation and IL-1β gene expression in the synovial tissue) was observed from 7 to 28 days, but not at 56 days. All of the inflamed synovium of the joint cannot be covered by the use of a US probe applied at the skin surface. Indeed, histologic evaluation of inflammation of synovial tissue in the femorotibial joint, where US was not administered, revealed no difference from that in the control group (data not shown). Another explanation is that 56 days (exactly 66 days after immunization) may be enough to

decrease the inflammation of synovial tissue in AIA naturally.

One hypothesis regarding the mechanism for the efficacy of this procedure is that the bioeffects are consequences of inertial cavitation, violent oscillations, and the collapse of bubbles in the surrounding fluid. The Optison stock concentration is ~6.5 × 10^8/ml, and 5% Optison (3.25 × 10^7/ml) was injected into the joint. The microbubbles consist of hollow albumin filled with octafluoropropane. They are collapsed by the cavitation produced by US, and are considered to be eliminated quickly by distribution or phagocytosis. Physical and chemical phenomena related to inertial cavitation include microstreaming, shock waves, microjets, extremely high localized temperatures, pressures inside the bubbles, and generation of free radicals (16). If US causes promotion of induction through increased membrane porosity, as described above, it is reasonable to expect that there would be some limitations for transducible agents in terms of molecular size, 3-dimensional structure, and chemical compositions. In this study, we chose MTX (MW 454.45) as a transducive agent. Because we showed that Texas Red–conjugated MTX (MW 1,257.49) was also incorporated into cells in an in vitro experiment, molecules of this size should be readily incorporated into cells with this method. Uptake into cells of some genes or other pharmacologic agents that have an antiinflammatory effect can be promoted by microbubble-enhanced US exposure.

In vivo US and Optison conditions were selected based on in vitro data, and it is clear that there are significant differences between in vitro and in vivo conditions. Since the power of US is reduced by the long distance between the joint and the skin in vivo, it may be necessary to elevate the US power to a higher setting, provided there is no resultant heat production on the skin. In this study, output power (1–2W), duration (30 seconds to 2 minutes), and duty cycle (10–50%) were elevated.

Electroporation is also an effective MTX transduction technique. It has been widely used for transduction of genes and pharmacologic agents in vivo and in vitro. It does not require viral vector construction or virus preparation. Many reports describe electroporation as a technique for promoting electrochemotherapy through the uptake of MTX into cancer cells (17–19). We also showed that electrochemotherapy was effective in digital chondrosarcoma (20). However, the electrical fields created also affect normal tissue beyond the target site. Furthermore, cell anomalies or tissue damage after electroporation have often been observed. Thus, it is not

an appropriate technique for the treatment of joints in RA patients. The encapsulation of MTX into cells with the use of a viral vector, recombinant polyomavirus–like particle, has been described (21), but this is a complex procedure and may not be suitable for clinical application.

MTX injection and US treatment can be used together in the clinic because of their low-risk safety profile. This technique may reduce synovitis in human arthritis and take the place of surgical synovectomy. It has been reported that surgical synovectomy of RA joints may offer short-term symptomatic relief but no retardation of the bone destruction or the disease process (22). While the benefits of our procedure might not match those of surgical excision of inflamed synovium, it is much less invasive than surgery and it can be performed frequently to obtain symptomatic relief. Further experiments are needed to determine whether this procedure alters the course of the disease. Furthermore, this technique can be applied in other inflammatory diseases.

For broader application in the clinic, there are some additional considerations that must be addressed. First, the intraarticular injection of MTX, which at high doses is sometimes used as an immunosuppressive agent, may cause adverse effects. The risk of iatrogenic infection warrants close attention. But MTX is reported to suppress production of superoxide and nitric oxide, and not to affect glycosaminoglycan synthesis of chondrocytes in vivo and in vitro (23,24).

Second, US may cause adverse effects. It has been reported that US increases matrix synthesis and that it does not affect the viability or proliferation of chondrocytes (25,26). The procedure reported here caused no harm to joint tissue apart from the proliferation zone in the synovium. However, the thick skin of the human joint may restrict the penetration of the ultrasonic vibration into synovial cells, which may cause a decrease in the uptake of MTX. The Sonitron is not approved for human use, but there is other equipment with greater power that is approved for human use in Japan (not for sonoporation). Longer exposure or higher power may cause local heat production. In such a case, a lower percentage setting of the duty cycle will help to prevent adverse effects. The optimal conditions necessary for the effective administration of US in humans need further investigation.

Third, the echo-contrast microbubbles may cause local or systemic side effects. These may include drug-induced allergic shock or joint pain because of high osmotic pressure. Moreover, another concern is that the overdosage of microbubbles or overexposure to ultra-

sonic waves may cause irreversible tissue injury. A minimum concentration of microbubbles would be desirable for clinical use. Optison has been used in the US and other countries for cardiac applications only, but it is not allowed for use in humans in some countries, such as Japan. Alternative clinical echo-contrast agents are now available in Japan. Levovist is one of these agents, although its gene transduction efficacy is reported to be inferior to that of Optison (27). Both are classified as second-generation microbubble agents. Optison consists of micrometer-sized (mean diameter 2–5 μm), denatured hollow albumin microspheres with a shell thickness of ~15 nm. The microbubbles are filled with octafluoropropane. Levovist is a galactose-based, air-filled microbubble agent, 99% of which is smaller than 7 μm. Further studies are planned to compare the performance of these agents in vivo.

This method can be used to introduce not only MTX but also other agents, such as steroids and some genes, into synovial cells. The procedure can be used not only for intraarticular injection but also for a systemic approach with intravenous or oral administration of the therapeutic drug. Studies are under way to examine these approaches. This technique enables a very targeted application of reagents to the diseased tissue, thus enabling healthy tissue to be spared from treatment.

REFERENCES

1. Hall GH, Jones BJ, Head AC, Jones VE. Intra-articular methotrexate: clinical and laboratory study in rheumatoid and psoriatic arthritis. Ann Rheum Dis 1978;37:351–6.
2. Marks JS, Stewart IM, Hunter JA. Intra-articular methotrexate in rheumatoid arthritis [letter]. Lancet 1976;2:857–8.
3. Franchi F, Seminara P, Codacci-Pisanelli G, Aronne T, Avella A, Bonomo L. Intra-articular methotrexate in the therapy of rheumatoid arthritis. Recenti Prog Med 1989;80:261–2.
4. Bertino JR, Goker E, Gorlick R, Li WW, Banerjee D. Resistance mechanisms to methotrexate in tumors [review]. Stem Cells 1996; 14:5–9.
5. Nakashima-Matsushita N, Homma T, Yu S, Matsuda T, Sunahara N, Nakamura T, et al. Selective expression of folate receptor β and its possible role in methotrexate transport in synovial macrophages from patients with rheumatoid arthritis. Arthritis Rheum 1999;42: 1609–16.
6. Ifergan I, Meller I, Issakov J, Assaraf YG. Reduced folate carrier protein expression in osteosarcoma: implications for the prediction of tumor chemosensitivity. Cancer 2003;98:1958–66.
7. Tachibana K, Uchida T, Ogawa K, Yamashita N, Tamura K. Induction of cell-membrane porosity by ultrasound [letter]. Lancet 1999;353:1409.
8. Kim HJ, Greenleaf JF, Kinnick RR, Bronk JT, Bolander ME. Ultrasound-mediated transfection of mammalian cells. Hum Gene Ther 1996;7:1339–46.
9. Ohta S, Suzuki K, Tachibana K, Yamada G. Microbubble-en-
hanced sonoporation: efficient gene transduction technique for chick embryos. Genesis 2003;37:91–101.
10. Hashiya N, Aoki M, Tachibana K, Taniyama Y, Yamasaki K, Hiraoka K, et al. Local delivery of E2F decoy oligodeoxynucleotides using ultrasound with microbubble agent (Optison) inhibits intimal hyperplasia after balloon injury in rat carotid artery model. Biochem Biophys Res Commun 2004;317:508–14.
11. Yamasaki K, Asai T, Shimizu M, Aoki M, Hashiya N, Sakonjo H, et al. Inhibition of NFκB activation using cis-element 'decoy' of NFκB binding site reduces neointimal formation in porcine balloon-injured coronary artery model. Gene Ther 2003;10:356–64.
12. Tachibana K, Tachibana S. The use of ultrasound for drug delivery [review]. Echocardiography 2001;18:323–8.
13. Kojima T, Mwale F, Yasuda T, Girard C, Poole AR, Laverty S. Early degradation of type IX and type II collagen with the onset of experimental inflammatory arthritis. Arthritis Rheum 2001;44: 120–7.
14. Sanchez-Pernaute O, Lopez-Armada MJ, Hernandez P, Palacios I, Navarro F, Martinez J, et al. Antifibroproliferative effect of tenidap in chronic antigen-induced arthritis. Arthritis Rheum 1997;40:2147–56.
15. Gibson UE, Heid CA, Williams PM. A novel method for real time quantitative RT-PCR. Genome Res 1996;6:995–1001.
16. Ward M, Wu J, Chiu JF. Experimental study of the effects of Optison concentration on sonoporation in vitro. Ultrasound Med Biol 2000;26:1169–75.
17. Hui SW. The application of electroporation to transfect hematopoietic cells and to deliver drugs and vaccines transcutaneously for cancer treatment [review]. Technol Cancer Res Treat 2002;1: 373–84.
18. Lin YC, Li M, Wu CC. Simulation and experimental demonstration of the electric field assisted electroporation microchip for in vitro gene delivery enhancement. Lab Chip 2004;4:104–8.
19. Weiss JM, Shivakumar R, Feller S, Li LH, Hanson A, Fogler WE, et al. Rapid, in vivo, evaluation of antiangiogenic and antineoplastic gene products by nonviral transfection of tumor cells. Cancer Gene Ther 2004;11:346–53.
20. Shimizu T, Nikaido T, Gomyo H, Yoshimura Y, Horiuchi A, Isobe K, et al. Electrochemotherapy for digital chondrosarcoma. J Orthop Sci 2003;8:248–51.
21. Abbing A, Blaschke UK, Grein S, Kretschmar M, Stark CM, Thies MJ, et al. Efficient intracellular delivery of a protein and a low molecular weight substance via recombinant polyomavirus-like particles. J Biol Chem 2004;279:27410–21.
22. Ochi T, Iwase R, Kimura T, Hirooka A, Masada K, Owaki H, et al. Effect of early synovectomy on the course of rheumatoid arthritis. J Rheumatol 1991;18:1794–8.
23. Hayem G, Domarle O, Thuong-Guyot M, Pocidalo JJ, Meyer O. Effects of methotrexate on the oxidative metabolism of cultured rabbit articular chondrocytes. J Rheumatol 2000;27:1117–20.
24. Neidel J, Sova L, Schroers B, Sintermann F, Manzke O, Bohlen H. It is effects of methotrexate on normal articular cartilage in vitro and in vivo. Ann Rheum Dis 1998;57:414–21.
25. Zhang ZJ, Huckle J, Francomano CA, Spencer RG. The effects of pulsed low-intensity ultrasound on chondrocyte viability, proliferation, gene expression and matrix production. Ultrasound Med Biol 2003;29:1645–51.
26. Zhang ZJ, Huckle J, Francomano CA, Spencer RG. The influence of pulsed low-intensity ultrasound on matrix production of chondrocytes at different stages of differentiation: an explant study [published erratum appears in Ultrasound Med Biol 2003;29: 1223]. Ultrasound Med Biol 2002;28:1547–53.
27. Li T, Tachibana K, Kuroki M, Kuroki M. Gene transfer with echo-enhanced contrast agents: comparison between Albunex, Optison, and Levovist in mice: initial results. Radiology 2003;229: 423–8.

© Springer-Verlag Tokyo 2005

ORIGINAL ARTICLE

Hiroshi Ohta · Shigeyuki Wakitani · Keiji Tensho
Hiroshi Horiuchi · Shinji Wakabayashi · Naoto Saito
Yukio Nakamura · Kazutoshi Nozaki · Yuuki Imai
Kunio Takaoka

The effects of heat on the biological activity of recombinant human bone morphogenetic protein-2

Abstract This study was designed to investigate effects of heat on the bone-inducing activity of recombinant human bone morphogenetic protein (rhBMP)-2. rhBMP-2 samples were heated at 50, 70, 90, or 100°C for 15 min, or 1, 2, 4, or 8 h, or autoclaved at 120°C for 15 min. The bone-inducing activity of the rhBMP-2 before and after heating was assayed in in vivo and in vitro systems. For the in vivo assay, 5 μg rhBMP-2 samples were impregnated into porous collagen disks (6 mm in diameter, 1 mm thickness), freeze dried, and implanted into the back muscles of ddY mice. Three weeks later, the implant was harvested from the host and examined for ectopic new bone tissue by radiography. The new bone mass was quantified by single-energy X-ray absorptiometry. The in vitro activity of the rhBMP-2 was assayed by adding the BMP sample at a concentration of 100 ng/ml to cultures of MC3T3-E1 cells. After 48 h, the alkaline phosphatase activity was measured. After heating at 50° or 70°C, no significant reduction in bone-inducing activity was noted in either in vivo or in vitro assay systems unless the protein was exposed to sustained heat at 70°C for 8 h, based on in vitro assay data. However, heating above 90°C and for longer periods led to a decrease in the biological activity of the rhBMP-2 in a time- and temperature-dependent manner. rhBMP-2 was rendered inactive when exposed to temperatures at or in excess of 120°C.

Key words Heat stability · Bone induction · Molecular structure

H. Ohta · S. Wakitani (✉) · K. Tensho · H. Horiuchi ·
S. Wakabayashi · N. Saito · Y. Nakamura
Department of Orthopaedic Surgery, Shinshu University School of
Medicine, 3-1-1 Asahi, Matsumoto 390-8621, Japan
Tel. +81-263-37-2659; Fax +81-263-35-8844

K. Nozaki
Applied Pharmacology Laboratories, Institute for Drug Discovery
Research, Yamanouchi Pharmaceutical, Tsukuba, Japan

Y. Imai · K. Takaoka
Department of Orthopaedic Surgery, Osaka City University
Graduate School of Medicine, Osaka, Japan

Introduction

Bone morphogenetic proteins (BMPs) belong to the transforming growth factor-β superfamily [1] and possess unique biologic activity that leads to new bone formation [2–4]. BMP-2 is a member of the BMP family, and the human form (hBMP) has been successfully synthesized by the use of DNA recombination technology (rhBMP) for commercial purposes. This protein is now being evaluated as a bone-graft substitute for the treatment of nonunion fractures, bone defect repairs, and spinal fusions [5–11]. In order to use rhBMPs clinically, it is necessary to understand how the molecular structure or bone-inducing activity of BMPs may be modified during transportation, storage, and intraoperative handling. In particular, the stabilization of BMP-retaining devices, or the use of BMP-2 in combination with heat-generating bone cement, are two instances where the stability of the protein would be challenged. Several authors have described the heat resistance of natural crude BMP extracted from the rat, rabbit, and human [12–16], but there has been little work done to look at the effects of heat on the stability and biological activity of rhBMP-2. This study describes how the biological activity and molecular structure of rhBMP respond to varying degrees of heat using in vivo and in vitro assay systems.

Materials and methods

Heat treatment of rhBMP-2

rhBMP-2 was provided by Yamanouchi Pharmaceutical (Tokyo, Japan) in a buffered solution (1 mg rhBMP-2/ml). This was diluted 3-fold (15 μl saline containing 5 μg rhBMP-2) and heated at 50, 70, 90, or 100°C for 15 min, or 1, 2, 4, or 8 h using a heat block (Dry Thermo Unit, Taitec, Saitama, Japan), or autoclaved at 120°C for 15 min. The biological activity of these heat-treated rhBMP-2 samples was then evaluated in in vitro and in vivo experiments to examine

changes in the biological activities of the rhBMP-2. As a control, rhBMP-2 that had not been exposed to heat was used in the assays.

Cell culture

A mouse osteoblastic cell line MC3T3-E1 was obtained from the RIKEN Cell Bank (Tsukuba Science City, Japan). These cells were seeded at a cell density of 3×10^5 cells/100-mm plastic dish and cultured with α-minimal essential medium (Gibco, Grand Island, NY, USA) supplemented with 10% (vol/vol) heat-inactivated fetal bovine serum (Gibco) at 37°C in an incubator with 95% humidified air and 5% CO_2.

Induction of alkaline phosphatase (ALP) by rhBMP-2

The biological activity of the rhBMP-2 was assayed based on the observation that BMP is capable of inducing expression of ALP in a dose-dependent manner. ALP activity is an early marker of osteoblastic differentiation [17]. The rhBMP-2 samples, heated as described above, were added to the MC3T3-E1 cells at a final concentration of 100 ng/ml. After 48 h, the osteoblastic cells were washed twice with phosphate-buffered saline, scraped from each well into 0.3 ml 0.5% NP-40 containing 1 mM $MgCl_2$ and 10 mM Tris (pH 7.5), and sonicated twice for 20 s with a sonicator (model W-220; Wakenyaku, Kyoto, Japan). The cell lysates were then centrifuged for 10 min at 3000 r.p.m., and the supernatants were used for the enzyme assay. ALP activity was assayed using the method of Kind–King [18] and a test kit (Alkaline Phospha K, Wako Pure Chemical Industries, Osaka, Japan) with phenylphosphate as a substrate.

The enzyme activity was expressed in King–Armstrong (K–A) units normalized to the protein content of the sample. The protein content was determined with a bicinchoninic acid protein assay kit (Pierce Chemical, Rockford, IL, USA) using bovine serum albumin as the standard. Each heat-treated rhBMP sample was measured in three separate dishes, and the ALP activity from each group was expressed as mean ± SD.

Preparation of BMP-containing collagen disks

In order to evaluate the influence of heating on the bone-inducing activities of the rhBMP-2, a classical in vivo experimental system of ectopic bone induction in mice was utilized. In this system, BMP was combined with collagen and implanted into muscle, whereupon an ectopic ossicle was elicited if the BMP was biologically active. In order to deliver the BMP, commercially available porous collagen sheets made from bovine Achilles tendon (Helistat Integra Life Sciences, Plainsboro, NJ, USA) were cut into round strips (6 mm in diameter, 1 mm thick), soaked in the sample solutions containing 5 µg of either the heated or nonheated control rhBMP-2, freeze-dried, and stocked at −20°C until implantation into mice.

Assay for the bone-inducing activities of heat-treated rhBMP-2

One hundred and seventy-six male ddY mice, 5 weeks of age, were purchased from Nippon SLC Co. (Shizuoka, Japan). The mice were housed in cages with free access to food and water for 1 week before the start of the experiment. Prior to surgery for implantation of the collagen/rhBMP-2 composite collagen disks, the mice were anesthetized with diethylether. The BMP-retaining pellets were implanted into the left dorsal muscle pouches (one pellet per animal). Twenty-two groups of mice (8 mice in each group) were implanted with collagen disks containing 5 µg rhBMP-2 that had never been heated (control), or heated at 50, 70, 90, or 100°C for 15 min, or for 1, 2, 4, or 8 h, or autoclaved at 120°C for 15 min. The mice were fed for 3 weeks and then killed. The implants were harvested and examined for ectopic new bone formation in situ by radiographic and histological methods. X-rays of the harvested tissues were taken with a soft X-ray apparatus (Sofron Co., Tokyo, Japan). In order to quantify the ectopically induced bony mass, the bone mineral content (BMC, mg) of each ossicle was measured by single-energy X-ray absorptiometry using a bone mineral analyzer (DCS-600; Aloka Tokyo, Japan). For the histology, the harvested tissue mass from each group was fixed in neutralized 10% formalin, defatted in chloroform, decalcified with 10% ethylenediamine tetraacetic acid, and embedded in paraffin wax. Sections of 5 µm thickness were cut, stained with hematoxylin–eosin, and observed under a light microscope.

All procedures for the animal experiments were carried out in compliance with the guidelines of the Institutional Animal Care Committee of Shinshu University.
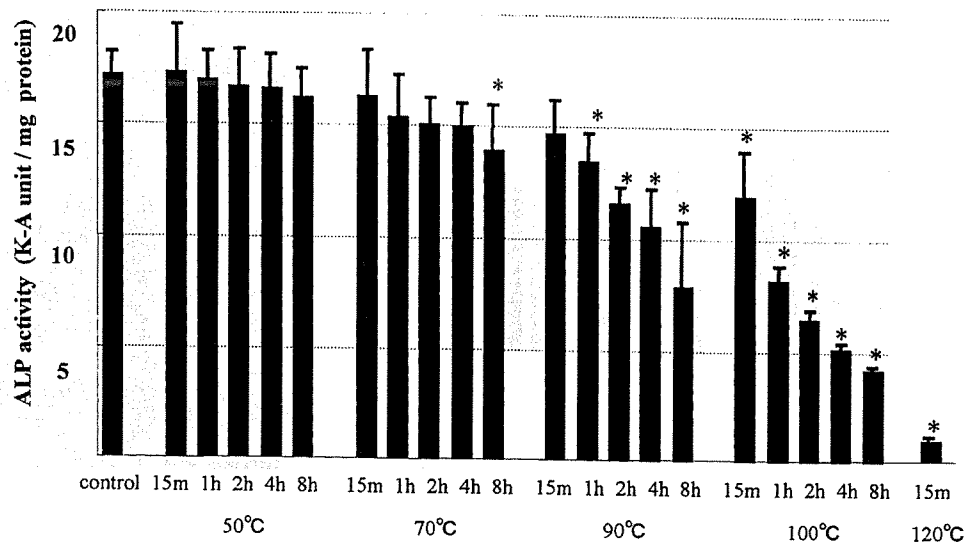
Sodium dodecyl sulfate-polyacrylamide gel electrophoresis (SDS-PAGE)

In order to examine the effects of heat on the rhBMP-2 molecules, heated or nonheated samples of the protein were electrophoresed on a SDS-PAGE slab gel. Five micrograms of nonheated rhBMP-2 or protein heated at 90°C on a heat block or at 120°C in an autoclave for 2 h were dissolved into 20 µl sample buffer solution (0.5 µM, pH6.8 Tris-HCl buffer solution/0.2% SDS/10% glycerol/0.01% bromophenol blue) with or without 100 mM dithiothreitol (DTT, a disulfide-bond reducing agent) and boiled for 5 min. Each sample was run on a SDS gel at 40 mA for 60 min. The gel was then stained with Comassie brilliant blue and destained in 10% acetic acid solution.
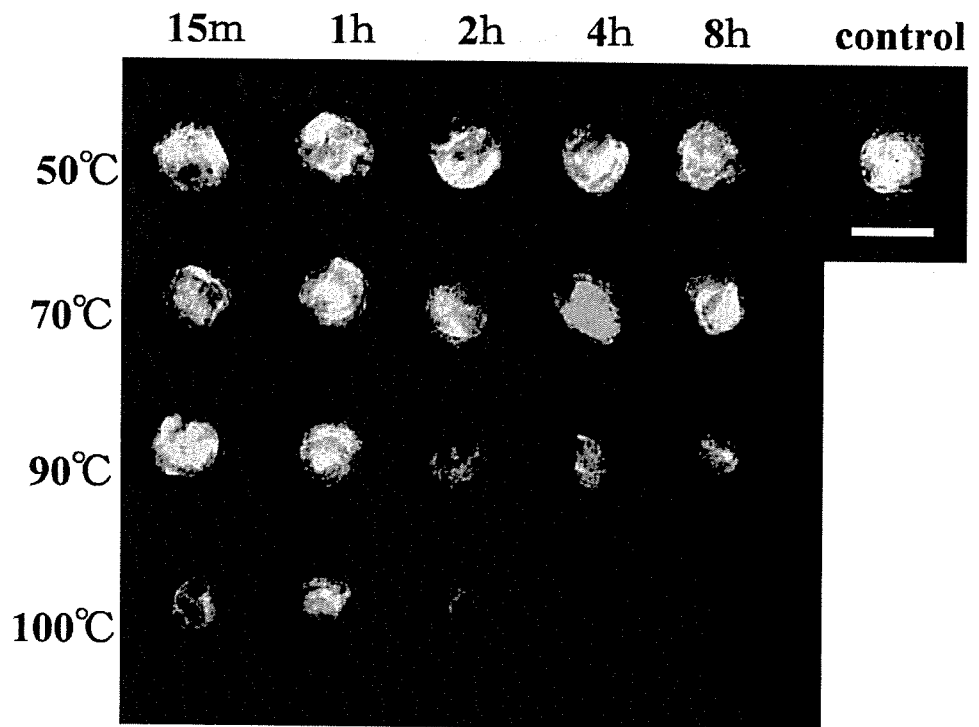
Statistical analysis

Quantitative data were expressed as the mean ± SD. Differences between control and experimental groups were considered to be statistically significant at $P < 0.05$ using the Kruskal–Wallis H-test with Bonferroni correction.

422

Results

Effects on ALP expression by heated rhBMP-2

Figure 1 shows the effects of the heat treatment on the
ALP-inducing activity of rhBMP-2 in MC3T3-E1 cells.
ALP-inducing activity was preserved at 50°C even after the
rhBMP-2 was heated at this temperature for 8 h. A notable
reduction in the ALP-inducing activity of rhBMP-2 was
seen using protein samples heated at 70°C for 8 h. At 90°C,
a significant reduction of activity was noted by heating
for 1 h or more in a time-dependent manner. By heating

at 100°C, the time-dependent reduction was profound.
The ALP-inducing activity was reduced to less than 1 unit/
mg protein when the rhBMP-2 was heated at 120°C for
15 min.

Change in the bone-inducing activity of rhBMP-2 by heating

Figure 2 shows representative ossicles elicited in mice
within a 3-week period by implanting collagen disks impreg-
nated with 5 μg rhBMP-2 heated at 50, 70, 90, or 100°C for
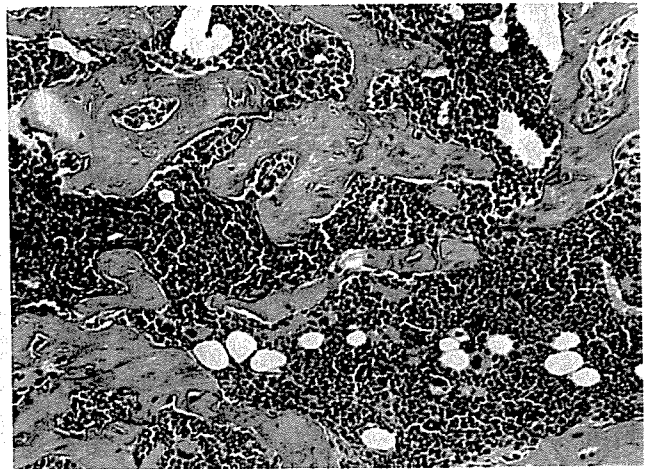15 min, or for 1, 2, 4, or 8 h. Ossicle size tended to become
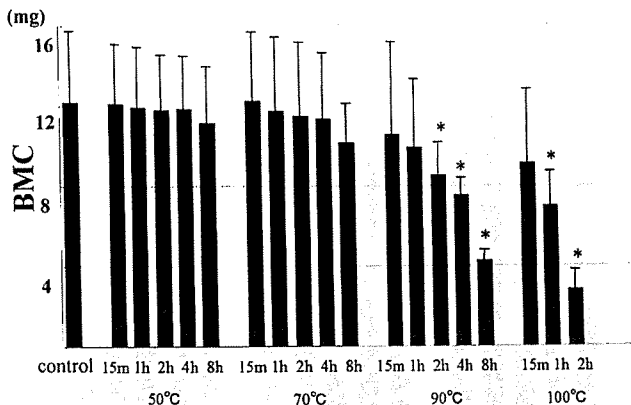
Fig. 3. The bone mineral content (*BMC*) of the tissues harvested at 3 weeks after surgery. Data are means ± SD of 8 samples. A significant difference from the control is indicated as * (*P* < 0.05). There was no significant difference between the BMC of the 50°C and 70°C groups and the control group. However, the mean BMCs of groups heated at 90°C for 2, 4, or 8 h and the one heated at 100°C for 1, or 2 h (*P* < 0.01) were significantly lower than that found in the control group. In the groups heated at 100°C for 4 h, at 100°C for 8 h, and at 120°C for 15 min, we found no evidence of new ectopic bone formation, as described in the legend to Fig. 2

Fig. 4. Photomicrograph of the tissue harvested at 3 weeks after implantation (heated to 50°C for 8 h) (H&E, ×200). Normal bone histology with hematopoietic marrow and bony trabeculae was observed

small when the rhBMP-2 was treated at 90°C for 2 h or more. After treatment for more than 4 h at 100°C or for 15 min at 120°C, the bone-inducing activity of rhBMP-2 was lost.

Figure 3 shows the mean BMC values of the ossicles from each of the groups. The mean (±SD) BMC of the control group was 12.2 ± 3.56 mg. In the group treated at 50°C for 8 h, the mean BMC was 11.2 ± 2.81 mg, which was not significantly lower than that of the controls. In the group with protein heated at 70°C, the mean BMC in the group treated at 70°C for 15 min was 12.2 ± 3.45 mg. The BMC in the 70°C group showed a downward trend, but no statistically significant difference was observed when compared with the control group. Similarly, in the group using protein heated at 90°C, the BMC of the harvested ossicles decreased with an extension of the heating time. The BMC of ossicles from the groups treated at 90°C for 15 min or 90°C for 1 h were not significantly different from those of the control group. However, the mean BMC values of the groups treated at 90°C for 2 h (8.48 ± 1.68 mg), at 90°C for 4 h (6.98 ± 1.06 mg), or at 90°C for 8 h (4.26 ± 0.53 mg) were significantly reduced when compared with those of the control group (*P* < 0.01). Again, in the group treated at 100°C for 15 min, the BMC was less than that of the controls, although there was no significant difference between the values. The mean BMC of the groups treated at 100°C for 1 h (6.96 ± 1.71 mg) or at 100°C for 2 h (2.80 ± 0.99 mg) were significantly lower than those from the control group (*P* < 0.01).

Histological analysis of the ossicles from all groups revealed normal bone histology with hematopoietic marrow and bony trabeculae (Fig. 4).

Changes in the SDS-PAGE profile of rhBMP-2 by heating

The SDS-PAGE profiles of rhBMP-2 before and after heating at 90 or 120°C are shown in Fig. 5. The original rhBMP-2 showed three dark bands at around 30-k Daltons (kD) and two light bands below 20 kD without DTT (lane 1). With DTT, the 30-kD bands became lighter and the lower molecular-sized bands became darker (lane 4). By heating at 90°C for 2 h, in the absence of DTT the 30-kD bands became a little indistinct and two lower sized bands disappeared (lane 2), and with DTT the 30-kD bands became lighter and the lower bands became darker (lane 5). By heating at 120°C for 2 h, in the absence of DTT the 30-kD bands remained although the three bands became indistinct (lane 3), and with DTT both of the 30-kD bands and the lower bands were lost (lane 6).

Discussion

BMPs (BMP-2, BMP-7) with potent bone-inducing activity have been successfully produced and developed for clinical use through DNA recombinant technology. Examples of clinical applications include the repair of damaged bone, the reconstruction of bone defects resulting from trauma, and resection of bone tumors. In terms of a successful clinical outcome, the bone-inducing activity of rhBMP-2 must be able to withstand the conditions associated with transportation and storage. In addition, rhBMP has to survive sterilization and the high temperatures encountered when implants are used in close contact with curing bone cement. Previous studies have qualitatively described the stable character of natural BMP based on the ability of crude insoluble BMP-retaining decalcified bone matrix to induce ectopic new bone. Nakanishi et al. [12] reported that rabbit bone-derived BMP extracts elicited ectopic bone after
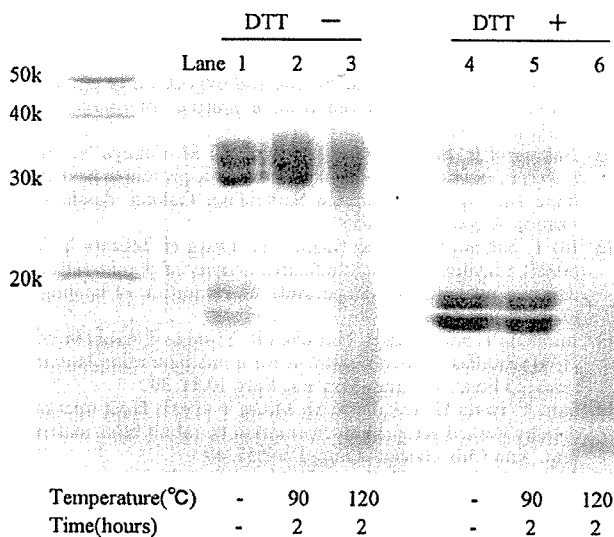
Fig. 5. SDS-PAGE profiles of rhBMP-2 before (*lane 1*) and after (*lane 2*) heating at 90°C and at 120°C (*lane 3*) for 2 h. *Lanes 4, 5,* and *6* show the respective samples under reducing conditions in the presence of dithiothreitol (DTT, a disulfide-bond reducing agent). The original rhBMP-2 showed three dark bands at around 30 k Daltons (kD) and two light bands below 20 kD without DTT (*lane 1*). With DTT, bands at 30 kD became lighter and the lower bands became darker (*lane 4*), which indicates that the dimers were reduced to monomers. By heating at 90°C for 2 h in the absence of DTT, the major 30-kD bands became a little indistinct, and the two lower-sized bands disappeared (*lane 2*). With DTT, bands at 30 kD became lighter and the lower bands became darker (*lane 5*), indicating that the bands at 30 kD without DTT maintained a dimeric structure. By heating at 120°C for 2 h, the original size of rhBMP-2 was maintained, although the three distinct bands were lost (*lane 3*). With DTT, both of the original 30-kD bands and those lower molecular-sized bands were lost (*lane 6*), indicating complete denaturation of the original configuration of the molecules

heating at 70°C for 10 min. However, the bone-inducing activity was lost when the sample was heated at over 100°C for 20 min. Some reports have also described similar results using crude BMP extracts as the bone-inducer in rodent models [13,14]. One report demonstrated that BMP activity was retained in a rabbit model after heating the matrix protein at 170°C for 10 min or at 140°C for 30 min [15].

In this study, the bone mineral content of the rhBMP-2-induced ossicles was used to evaluate the bone-inducing activity of the heat-treated rhBMP-2 in an in vivo system. In addition, the ability of rhBMP-2 to induce ALP activity in osteoblastic cells in culture was used as a model to confirm the results from the in vivo experiments. The ALP-inducing activity of the rhBMP-2 was little affected by heat treatment up to 70°C for 8 h or up to 90°C for 1 h, but then decreased gradually with increasing temperature and time. The ALP-inducing activity was eventually lost after heating the rhBMP-2 at 120°C, a treatment that denatured the molecular structure of the rhBMP-2 as shown on a SDS-PAGE profile. These results were in accordance with the in vivo results, and suggest that rhBMP-2 is largely stable in nature. The use of autopolymerising polymethylmethacrylate (PMMA)-based bone cement is the most common method

chosen for prosthetic component fixation in total joint replacement surgery. During the polymerization of PMMA, high peak temperatures are reached. The temperature peak ranges from 48°C to 105°C at the bone–cement interface, and from 80°C to 124°C in the cement. The exposure time over 50°C is reported to be between 30 and 400 s [19]. Thus, the data from the present study suggest that contact with curing bone cement would not affect the bone-inducing activity of rhBMP-2. Sterilizing by autoclave (120°C) would effectively inactivate the biological action of this protein, but sterilizing by ethylene oxide gas (60°C for 3 h or 40°C for 6 h) would not, as reported previously [20].

The heat-stable character of BMP may be derived from its molecular structure. It is known that the bioactive BMP-2 molecule consists of a homodimer which is essential for its biological activity. The homodimer consists of two 114 amino acid monomers with 7 cysteine residues that form three intramolecular disulfide bonds, with one intermolecular disulfide bond forming a cysteine knot [21]. The heat-resistant nature of the BMP might be explained by the cysteine-knot formation, which is known to contribute to the structural stability of the protein.

The biological activity of the rhBMP was reduced following heat denaturation at 90°C for 2 h as evaluated in an in vivo assay system, and for 1 h in an in vitro assay system. At these higher temperatures, the reduction in rhBMP-2 activity was temperature- and time-dependent. In order to visualize the heat-dependent changes in molecular structure, changes in the SDS-PAGE gel profile after heating were observed. As previously described, the rhBMP-2 molecule has a molecular size of around 16 kD with one N-glycosylation site, and it forms a homodimer which has biological activity [6–8,22]. Therefore, the three bands at 30 kD in the control lane on the SDS-PAGE with no disulfide bond reduction indicated dimeric BMP-2 molecules with 2, 1, or no sugar chains, respectively (see Fig. 5). Further, the two faint bands below 20 kD were monomers with or without glycosylation because of their similarity to the molecular sizes of the DTT-reduced rhBMP-2 monomer. By heating at 90°C for 2 h, in the absence of DTT the dimer bands became a little indistinct and the monomer bands were lost, which indicated complete deformation of the rhBMP-2 monomer. With DTT, the dimer bands became lighter and the monomer bands became darker. These changes most likely reflect partial deformation of the original three-dimensional configuration of the rhBMP-2 dimers, which corresponds with the partial loss of bone inducing activity. A higher temperature (120°C for 2 h) made the dimer bands more indistinct and eventually degraded the structure of the monomers, as seen on DTT-reduced SDS-PAGE, with the resultant loss of biological activity.

In conclusion, the biological activity and molecular structure of rhBMP-2 were shown to be fairly resistant to heat treatment. In considering the potential clinical uses of rhBMP-2, the stable character of the protein suggests that it would not need to be cooled during transportation or storage. In addition, it was found that contact with heated material such as curing bone cement would not affect the

bone-inducing activity of the rhBMP-2. However, the autoclaving of rhBMP-2 causes this protein to lose its biological activity based on the results of the present study.

References

1. Celeste AJ, Iannazzi JA, Taylor RC, Hewick RM, Rosen V, Wang EA, Wozney JM (1990) Identification of transforming growth factor beta family members present in bone-inductive protein purified from bovine bone. Proc Natl Acad Sci USA 87:9843–9847
2. Urist MR (1965) Bone formation by autoinduction. Science 150:893–899
3. Urist MR, Iwata H (1973) Preservation and biodegradation of the morphogenetic property of bone matrix. J Theor Biol 38:155–167
4. Reddi AH, Anderson WA (1976) Collagenous bone matrix-induced endochondral ossification hemopoiesis. J Cell Biol 69:557–572
5. Sampath TK, Muthukumaran N, Reddi AH (1987) Isolation of osteogenin, an extracellular matrix-associated, bone-inductive protein, by heparin affinity chromatography. Proc Natl Acad Sci USA 84:7109–7113
6. Wozney JM, Rosen V, Celeste AJ, Mitsock LM, Whitters MJ, Kriz RW, Hewick RM, Wang EA (1988) Novel regulators of bone formation: molecular clones and activities. Science 242:1528–1534
7. Wang EA, Rosen V, Cordes P, Hewick RM, Kriz MJ, Luxenberg DP, Sibley BS, Wozney JM (1988) Purification and characterization of other distinct bone-inducing factors. Proc Natl Acad Sci USA 85:9484–9488
8. Wang EA, Rosen V, D'Alessandro JS, Bauduy M, Cordes P, Harada T, Israel DI, Hewick RM, Kerns KM, LaPan P, Luxenberg DH, McQuid D, Moutsatsos IK, Nove J, Wozney JM (1990) Recombinant human bone morphogenetic protein induces bone formation. Proc Natl Acad Sci USA 87:2220–2224
9. Wozney JM (1992) The bone morphogenetic protein family and osteogenesis. Mol Reprod Dev 32:160–167
10. Takaoka K, Yoshikawa H, Hashimoto J, Miyamoto S, Masuhara K, Nakahara H, Matsui M, Ono K (1993) Purification and characterization of a bone-inducing protein from a murine osteosarcoma (Dunn type). Clin Orthop 292:329–336
11. Takaoka K, Yoshikawa H, Hashimoto J, Masuhara K, Miyamoto S, Suzuki S, Ono K, Matsui M, Oikawa S, Tsuruoka N, Tawaragi Y, Inuzuka C, Katayama T, Sugiyama M, Tsujimoto M, Nakanishi T, Nakazatio H (1993) Gene cloning and expression of a bone morphogenetic protein derived from a murine osteosarcoma. Clin Orthop 294:344–352
12. Nakanishi K, Sato K, Sato T, Takahashi M, Fukaya N, Miura T (1992) Preservation of bone morphogenetic protein in heat-treated bone (in Japanese). Nippon Seikeigeka Gakkai Zasshi (J Jpn Orthop Assoc) 66:949–955
13. Ito T, Sakano S, Sato K, Sugiura H, Iwata H, Murata Y, Seo H (1995) Sensitivity of osteoinductive activity of demineralized and defatted rat femur to temperature and duration of heating. Clin Orthop 316:267–275
14. Inokuchi T, Ninomiya H, Hironaka R, Yoshida S, Araki M, Sano K (1991) Studies on heat treatment for immediate reimplantation of resected bone. J Cranio-Max-Fac Surg 19:31–39
15. Sato T, Iwata H, Takahashi M, Miura T (1993) Heat tolerance of activity toward ectopic bone formation by rabbit bone matrix protein. Ann Chir Gynaecol Suppl 207:37–40
16. Izawa H, Hachiya Y, Kawai T, Muramatsu K, Narita Y, Ban N, Yoshizawa H (2001) The effect of heat-treated human bone morphogenetic protein on clinical implantation. Clin Orthop 390:252–258
17. Dunlop LL, Hall BK (1995) Relationships between cellular condensation, preosteoblast formation and epithelial-mesenchymal interactions in initiation of osteogenesis. Int J Dev Biol 39:357–371
18. Kind PRN, King EJ (1954) Estimation of plasma phosphatase by determination of hydrolyzed phenol with amino-antipyrine. J Clin Pathol 7:322–326
19. Borzacchiello A, Ambrosio L, Nicolais L, Ronca D, Guida G (2001). The temperature at the bone–cement interface: modeling and in vitro analysis. In: Pipino F (ed) Bone Cement and Cemented Fixation of Implants. Zenit, Rome, p 135–140
20. Nawata M, Wakitani S, Nakaya H, Tanigami A, Seki T, Nakamura Y, Saito N, Sano K, Hidaka E, Takaoka K (2005). Use of bone morphogenetic protein-2 and diffusion chambers to engineer cartilage tissue for the repair of defects in articular cartilage. Arthritis Rheum 52:155–163
21. Scheufler C, Sebald W, Hulsmeyer M (1999) Crystal structure of human bone morphogenetic protein-2 at 2.7-A resolution. J Mol Biol 287:103–115
22. Wozney JM (1989) Bone morphogenetic proteins. Prog Growth Factor Res 1:267–280

ORIGINAL ARTICLE

Yukio Nakamura · Shigeyuki Wakitani · Naoto Saito
Kunio Takaoka

Expression profiles of BMP-related molecules induced by BMP-2 or -4 in muscle-derived primary culture cells

Abstract The formation of ectopic bone in muscle following the implantation of decalcified bone matrix led to the search and eventual discovery of bone morphogenetic proteins (BMPs) in bone matrix. The precise sequence of molecular events that underpin the cellular transformation of undifferentiated mesenchymal cells into bone has not been established, and is the subject of this study. Northern and Western blot analyses were used to examine changes in gene expression of cells treated with BMP-2 or -4. The molecules, which included BMP receptors (BMPRs), Noggin (a BMP-specific antagonist), osteocalcin (OC), Smad-4, and MyoD, were examined at messenger RNA (mRNA) and protein levels. The changes in expression of these molecules were followed in mouse muscle-derived primary culture cells, and osteoblastic or nonosteoblastic embryonic cell lines. We show the early up-regulation of BMPR-1A, -2, Noggin, OC, and Smad-4 in muscle-derived primary culture cells in a dose-dependent manner in response to BMP-2 or -4. MyoD expression was not detected after BMP stimulation. The differential expression of these positive and negative regulators of BMP signaling points to a potential regulatory mechanism for bone induction in mesenchymal cells.

Key words BMP signaling · Feedback · Mesenchymal cells · Muscle · Up-regulation

Introduction

Bone morphogenetic proteins (BMPs) are multifunctional cytokines belonging to the transforming growth factor-β

Y. Nakamura (✉) · S. Wakitani · N. Saito
Department of Orthopaedic Surgery, Shinshu University School of Medicine, 3-1-1 Asahi, Matsumoto 390-8621, Japan
Tel. +81-263-37-2659; Fax +81-263-35-8844

K. Takaoka
Department of Orthopaedic Surgery, Osaka City University Hospital, Osaka, Japan

(TGF-β) superfamily. Among the BMP family, BMP-2, -4, and -7 (osteogenic protein-1) have been recognized as potent bone inducers [1–3], and BMP-2 and -4 also play critical roles in early embryogenesis and skeletal development [4]. Signaling by BMPs requires binding of the BMP (BMP-2, -4, and -7) molecules to the BMP receptors (BMPRs), which consist of two different types of serine-threonine kinase receptors, known as BMP type 1 receptors (1A and 1B) and BMP type 2 receptor [5]. These receptors then phosphorylate intracellular proteins such as the Smad-1 or -5 to effect intracellular signaling and physiological responses [6–9]. Therefore, BMPR expression is a prerequisite for the biological action of the BMPs [1–5]. BMP action may also be modulated by a group of BMP-binding proteins outside the responding cells. Noggin is a representative molecule with such a function, and is assumed to contribute to the negative regulation of BMP action or bone formation under physiological conditions [6–9].

Changes in expression of those molecules involved in BMP signaling are critical to understanding the mechanism of BMP-induced osteogenic differentiation and feedback mechanisms following treatment with BMPs. We previously examined an ectopic bone-forming model in mice [10], and found that BMPR-1A, -2, and Noggin were induced by BMP-2 in muscle tissues during the early phase of the reaction. To confirm this mechanism in in vitro systems, we used muscle-derived primary culture cells, and osteoblastic or non-osteoblastic embryonic cell lines were used as controls.

Materials and methods

Recombinant human BMP-2 (rhBMP-2) and mouse BMP-4 (mBMP-4)

rhBMP-2 was produced by the Genetics Institute (Cambridge, MA, USA) using DNA recombination techniques, and donated to us through Yamanouchi Pharmaceutical (Tokyo, Japan), as described elsewhere [11].

Conditioned media of mBMP-4-transfected Chinese hamster ovary (CHO) cells (BMP-CHO) were the source of mBMP-4. Details of the BMP-CHO cells have been described previously [12,13]. In mBMP-4-conditioned media, the alkaline phosphatase activity of the 10% conditioned media corresponds to approximately 70 ng/ml rhBMP-2 [13]. The BMP-CHO cells transfected with mBMP-4 cDNA or mock vector (for a control) were propagated at a density of 1×10^6 cells/100-mm plastic dish (Falcon no. 3003; Becton Dickinson Labware, Tokyo, Japan), and were then cultured in 10 ml Dulbecco's modified Eagle's medium (DMEM; Gibco-BRL, Grand Island, NY, USA) with 10% fetal calf serum (FCS; Sigma Chemical, St. Louis, MO, USA) at 37°C for 5 days. The conditioned media were collected after 5 days and stored at 4°C.

Cell culture

Muscle-derived primary culture cells were prepared from the thigh muscles of newborn ddy mice (Nippon SLC, Shizuoka, Japan), as described previously [14], and cultured on a 100-mm plastic dish in DMEM containing 10% (vol/vol:v/v) heat-inactivated FCS and penicillin-streptomycin (PSM) antibiotic mixture (Invitrogen). A murine osteoblastic cell line, MC3T3-E1, and murine embryonic fibroblast-like cell line, NIH3T3, were obtained from the RIKEN Cell Bank (Tsukuba, Japan) and cultured on a 100-mm plastic dish in α-minimal essential medium (Gibco-BRL) and DMEM, respectively, containing 10% (v/v) heat-inactivated FCS.

Experimental protocols

To examine the effects of rhBMP-2 and mBMP-4 on the expression of BMPRs, Noggin, OC, Smad-4, and MyoD in muscle-derived primary culture cells, and MC3T3-E1 and NIH3T3 cells, the culture media were replaced with fresh media containing rhBMP-2 or mBMP-4 at various concentrations (0, 10, 100, 500, 1000, or 1500 ng/ml for rhBMP-2, and 0%, 10%, 20%, 40%, 60%, or 80% conditioned media for mBMP-4). The cells were cultured at 37°C in a humidified 5% CO_2 incubator for a period of 6 days, with a change of media on day 3. Cells cultivated for 0, 12, 24, 48, 72, 96, 120, or 144 h with each medium containing rhBMP-2 (0, 10, 100, 500, 1000, or 1500 ng/ml) or mBMP-4 (0%, 10%, 20%, 40%, 60%, or 80%) were collected and processed for Northern blot analysis. Cells cultivated for 24, 48, 72, or 96 h with each medium containing rhBMP-2 (1000 or 1500 ng/ml) or mBMP-4 (60% or 80%) were collected and processed for Western blot analysis, as described below.

RNA preparation and reverse transcriptase-polymerase chain reaction (RT-PCR)

Total RNA from primary culture cells derived from embryonic mouse thigh muscle and MC3T3-E1 and NIH3T3 cells was extracted using Isogen (Nippon Gene, Tokyo, Japan)

according to the manufacturer's instructions. After treating with RNase-free deoxyribonucleases II (Gibco-BRL), complementary DNA (cDNA) was synthesized using an RNA polymerase chain reaction (PCR) kit (Takara Shuzo, Ohtsu, Japan) according to the manufacturer's instructions. The reaction time was 30 min at 42°C. Aliquots of the cDNA pool obtained were subjected to PCR and amplified in a 20 μl reaction mixture using Taq polymerase (Takara Shuzo). Amplifications were performed in a Program Temp Control System (PC800; ASTEC, Fukuoka, Japan) for 30 cycles after an initial denaturation step at 94°C for 3 min, denaturation at 94°C for 30 s, annealing for 30 s at 60°C, and extension at 72°C for 90 s, with a final extension at 72°C for 10 min. Reaction products were electrophoresed in a 1.5% agarose gel, and the amplified DNA fragments were visualized by ethidium bromide staining under UV light. PCR products were subcloned and sequenced using a DNA sequencing kit (Applied Biosystems, Warrington, UK). The primers of Noggin, Smad-4, OC, and MyoD for PCR were set as described previously [10,13,15]. The primers of BMPRs for PCR were set as follows: BMPR-1A, 5'-CTCATGTTCAAGGGCAG-3' (5' sense) and 5'-CCCCTGCTTGAGATACTC-3' (3' antisense; 346–362 and 850–833, respectively); BMPR-1B, 5'-ATGTGGG CACCAAGAAG-3' and 5'-CTGCTCCAGCCCAATGC T-3' (215–231 and 681–664, respectively); BMPR-2, 5'-GTGCCCTGGCTGCTATGG-3' and 5'-TGCCGCCTC CATCATGTT-3' (47–64 and 592–575, respectively). Nucleotide sequences of the cDNA fragments were checked and found to be identical to mouse BMPRs (BMPR-1A, NM009758; BMPR-1B, NM007560; BMPR-2, NM007561). The specificity of these cDNAs was confirmed by sequencing using an autosequence analyzer (ABI Prism 310 Genetic Analyzer; Perkin-Elmer Japan, Tokyo, Japan).

Northern blot analysis

Twenty micrograms of total RNA were separated by electrophoresis on a 1.0% agarose–formaldehyde gel and blotted onto Hybond-N^+ membrane (Amersham Intl., Piscataway, NJ, USA) for Northern blotting. Filters were hybridized overnight with random-primed [^{32}P]-labeled mouse BMPRs, Noggin, OC, Smad-4, and MyoD cDNA fragment probes at 65°C for 3 h in hybridization buffer (50 mM Tris-HCl (pH 7.5), 1 mg/ml denatured salmon sperm DNA, 1% SDS, 1 M NaCl, 10 mM EDTA, 0.2% Ficol 400, 0.2% polyvinylpyrolidone, and 0.2% bovine serum albumin) and washed three times with 0.1 × SSC and $NaDodSO_4$ for 1 h at 68°C. The signals were detected by a BioImaging Analyzer BAS-1500 (Fuji Photo Film, Tokyo, Japan). For reprobing, each hybridized probe was removed by boiling the membrane in 0.5% SDS, and then sequentially hybridized with the respective target probes.

Western blotting

Muscle-derived primary culture cells, MC3T3-E1 cells, NIH3T3 cells, and mouse skeletal muscle tissue (as a posi-

tive control) were homogenized and dissolved in 0.5ml sample buffer (0.05M Tris-HCl (pH 6.8), 2% SDS, 6% β-mercaptoethanol, and 10% glycerol) and centrifuged at 12000g for 5min at 4°C. The supernatant was used as the sample, and the protein content of each sample was measured by UV assay at an OD of 280nm. Anti-mouse Noggin antibody (R&D Systems, Minneapolis, MN, USA) was used at 1μg/ml. Polyclonal goat antibodies for BMPRs (Santa Cruz, San Diego, CA, USA) were also used at a dilution of 1μg/ml. Aliquots of protein solution (5μl) were adjusted to 1μg/μl, mixed with 1% BPB (1μl), and then boiled for 2min and loaded onto each lane of SDS (10%–20%) acrylamide gradient gels (35mA, low voltage, 90min). After running the gels, BMPR-1A, -1B, -2, and Noggin proteins in mouse embryo muscle-derived cells, and MC3T3-E1 and NIH3T3 cells, and mouse skeletal muscle tissue were stained with Coomassie brilliant blue (Sigma Chemical). The protein bands were then transferred to polyvinylidene difluoride membrane (Immunobilon-P Transfermembrane, Millipore, Bedford, MA, USA) according to the manufacturer's instructions. After treatment with Blocking Reagent (Nippon Roche, Tokyo, Japan) for 1h at room temperature, the membranes were washed with PBS for 5min, and then incubated for 1h with primary antibody (BMPRs, 1:200; Noggin, 1:100). After two 5-min washes with PBS, the membranes were incubated with peroxidase-conjugated rabbit anti-goat antibody (1:50; Histofine, Nichirei, Tokyo, Japan) for 1h. After two further 5-min washes with PBS, the immunoblot was developed using an ImmunoStar Kit for Rabbit (Wako Pure Chemical Industries, Tokyo, Japan) to detect biotin and chemiluminescence.

Results

Expression level of messenger RNA (mRNA)

The increase in transcription of BMPR-1A, -2, Noggin, OC, and Smad-4 appeared to be dose-dependent. The expression pattern of these molecules in muscle-derived primary culture cells after 24h stimulation by rh-BMP-2 or mBMP-4 is shown in Fig. 1. When we performed Northern blotting on all cell sources using 0, 10, 100, 500, 1000, and 1500ng/ml doses of rhBMP-2, or 0%, 10%, 20%, 40%, 60%, and 80% doses of mBMP-4, the gene expression levels of these molecules were the similar at the following doses: rhBMP-2 (1000ng/ml), rhBMP-2 (1500ng/ml), or mBMP-4 (60%) and mBMP-4 (80%). Therefore, the expression of BMPR-1A, -2, Noggin, OC, and Smad-4 appeared to reach a plateau at the 1000ng/ml dose of rhBMP-2 and 60% mBMP-4. The mRNA expression of these molecules was readily detected at the 10ng/ml dose of rhBMP-2 and 10% mBMP-4 (Figs. 1 and 2).

The expression levels of BMPR-2 and Noggin mRNA were sharply elevated on day 1, and then decreased gradually in the muscle-derived primary culture cells at all concentrations. Representative expression patterns using rhBMP-2 (100ng/ml) or mBMP-4 (20%) are shown in Figs.

3A and 4A. BMPR-1A transcription was also elevated on day 1, but at lower levels when compared with BMPR-2 at all concentrations (Figs. 3 and 4).

Similar patterns for BMPR-1A, -2, and Noggin were observed in MC3T3-E1 and NIH3T3 cell lines, but to a much lower degree than that seen in the muscle-derived primary culture cells at all concentrations. The typical expression figures using rhBMP-2 (1000ng/ml) or mBMP-4 (60%) in MC3T3-E1 and NIH3T3 cell lines are shown in Figs. 5–8. BMPR-1B expression was not detected by Northern blotting before or after BMP stimulation in any cell sources examined, or in OC later on day 4. The Smad-4 mRNA level gradually increased, and reached a plateau from day 2 (Figs. 5–8).

MyoD mRNA expression was detected without BMP-2 or -4 exposure throughout the experimental period. A typical figure in which muscle-derived primary culture cells were stimulated by BMP-2 or -4 after 24h is shown in Fig. 9A or 9B.
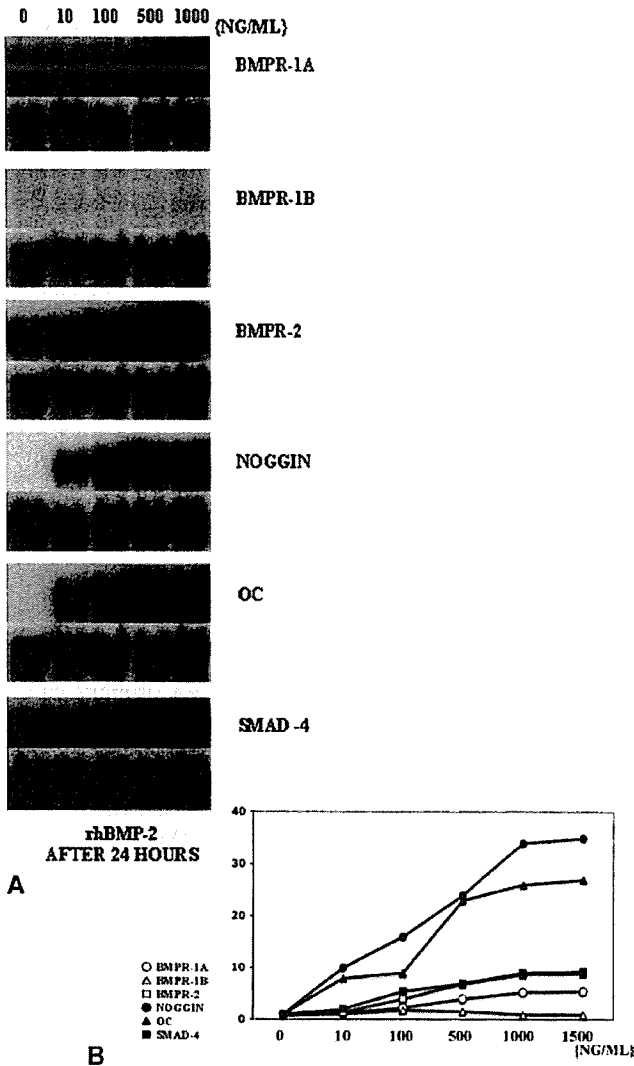
Protein expression levels

Western blotting on the muscle-derived primary culture cells using either 1000 or 1500ng/ml doses of rhBMP-2, or 60% or 80% of mBMP-4, revealed that the protein expression levels of BMPR-1A, -2, and Noggin were the same at the 1000ng/ml and 1500ng/ml doses of rhBMP-2, and at 60% or 80% concentrations of mBMP-4. Therefore, rhBMP-2 (1000ng/ml) or mBMP-4 (60%) was used for all subsequent studies of protein expression levels in the muscle-derived primary culture cells (Fig. 10). We did not perform Western blotting on MC3T3-E1 and NIH3T3 cell lines because of the weak expression revealed by Northern blotting.

The translational expression levels of BMPR-1A, -2, and Noggin were enhanced on day 2 and then decreased gradually in the muscle-derived primary culture cells. BMPR-1B expression was not detectable by Western blotting before or after BMP stimulation in the muscle-derived primary culture cell (Fig. 10).
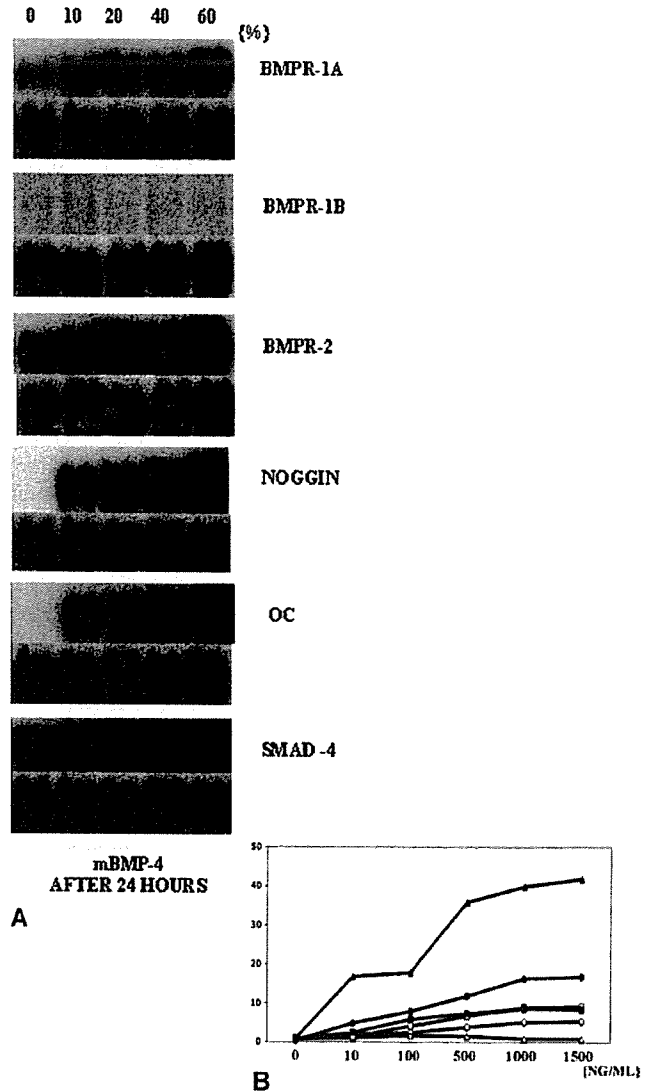
Discussion

This study showed increased transcription and translation of BMPR-1A, -2, and Noggin and increased transcription of OC and Smad-4 in response to rhBMP-2 or mBMP-4 in muscle-derived primary culture cells. Clearly, the muscle-derived primary culture cells are capable of responding to changes in the external concentrations of the bone growth factors. Induction of BMPR-1A and -2 following exposure to BMPs points to the activation of a receptor-mediated pathway to effect intracellular signaling by these molecules. Although the reason for the predominant induction of BMPR-2 among BMPRs is unknown at present, it is possible that an increased number of BMPR-2 molecules with a high affinity for BMP might allow greater capture of this

Fig. 1. Gene expression level of BMPR-1A, -1B, -2, Noggin, OC, and Smad-4 after 24-h stimulation of rhBMP-2 (0, 10, 100, 500, 1000 ng/ml) in muscle-derived primary culture cells by Northern blot analysis (A) and quantitation of the data of Northern blot analysis by Densitometry (B). G3PDH mRNA levels (the bottoms of all lanes are G3PDH) obtained by Northern blotting were used for normalization (A). The score on hour 0 (just after BMP stimulation) was used as a standard (B). BMPR-1A, -2, Noggin, OC, and Smad-4 were up-regulated dose-dependently. No increase in BMPR-1B expression was observed during the course of the study. The expression levels of these molecules were almost the same using 1000 ng/ml and 1500 ng/ml rhBMP-2 (1500 ng/ml rhBMP-2 data not shown in Fig. 1A)

Fig. 2. Gene expression level of BMPR-1A, -1B, -2, Noggin, OC, and Smad-4 after 24-h stimulation of mBMP-4 [0%, 10%, 20%, 40%, and 60% (v/v) conditioned media] in muscle-derived primary culture cells by Northern blot analysis (A) and quantitation of the data of Northern blot analysis by Densitometry (B). G3PDH mRNA levels (the bottoms of all lanes are G3PDH) obtained by Northern blotting were used for normalization (A). The score on hour 0 (just after BMP stimulation) was used as a standard (B). The gene expression pattern of the molecules after stimulation of mBMP-4 was similar to that observed after stimulation of rhBMP-2. The expression levels of these molecules were almost the same using 60% and 80% mBMP-4. (80% mBMP-4 data not shown in Fig. 2A)

ligand and subsequent activation of BMPR-1A for enhanced transduction of the BMP signal into cells.

We have observed that expression of BMPR-1A and -2 is significantly increased during the early phase of ectopic bone formation following the implantation of rhBMP-2 into the back muscles of adult mice [10]. Based on these data from in vivo and in vitro studies, the activation of BMPR-1A after BMPR-2 might be a key event following BMP stimulation of muscle tissue. BMPR-1A, -2, and Noggin were induced in MC3T3-E1 and NIH3T3 cell lines, but to a

much lesser degree than that seen in the muscle-derived primary culture cells used in this study.

A specific role of BMPR-1B in skeletal development has been proposed based on the abnormal interphalangeal joint formation in an animal with a null mutation in this receptor. However, the expression of BMPR-1B appeared to be limited in the muscle-derived primary culture cells and the osteoblastic or nonosteoblastic embryonic cell lines, even after exposure to BMPs [16–19]. The lack of expression of BMPR-1B was in accordance with results in a previous

430
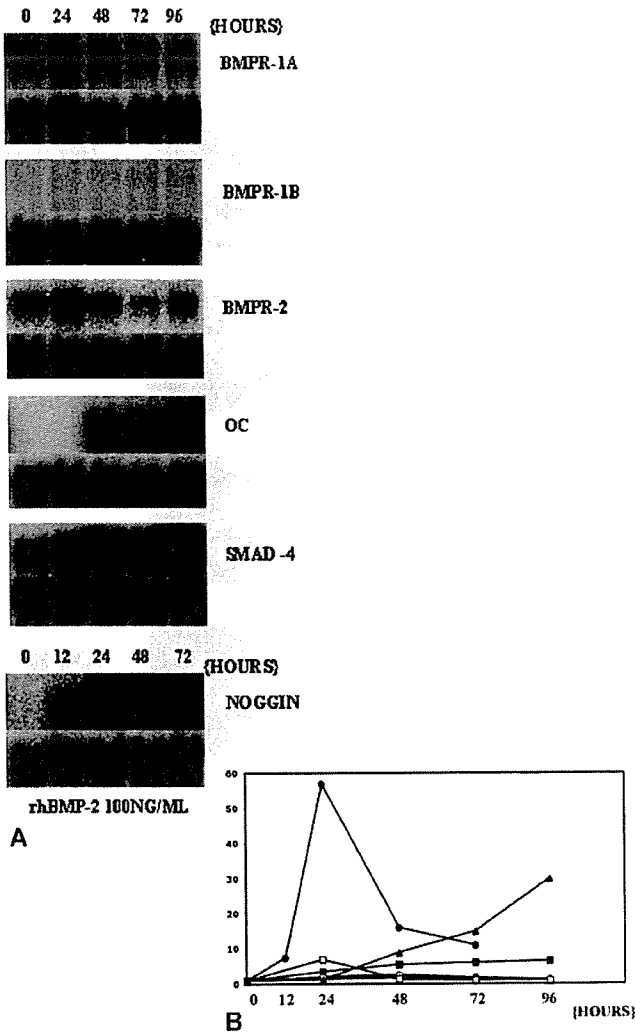
Fig. 3. Gene expression of BMPR-1A, -1B, -2, OC, and Smad-4 for 0, 24, 48, 72, and 96 h and Noggin for 0, 12, 24, 48, and 72 h after 100 ng/ml rhBMP-2 stimulation in muscle-derived primary culture cells by Northern blot analysis (A) and quantitation of the data of Northern blot analysis by Densitometry (B). G3PDH mRNA levels (*the bottoms of all lanes* are G3PDH) obtained by Northern blotting were used for normalization (A). The score on hour 0 (just after BMP stimulation) was used as a standard (B). After rhBMP-2 stimulation, OC was up-regulated time-dependently. Noggin level peaked at 24 h. Expression of BMPR-1A and -2 was increased moderately after 24 h, then gradually decreased thereafter. Smad-4 was gradually and weakly up-regulated after stimulation. BMPR-1B was not increased during the experimental period
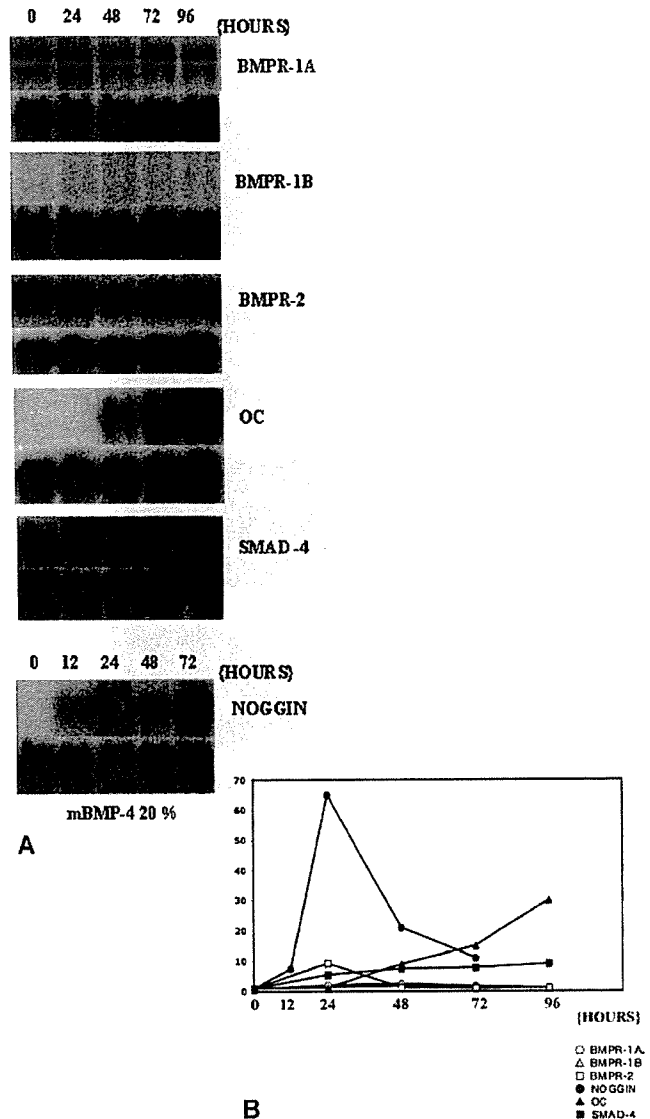
Fig. 4. Gene expression of BMPR-1A, -1B, -2, OC, and Smad-4 for 0, 24, 48, 72, and 96 h and Noggin for 0, 12, 24, 48, and 72 h after 20% mBMP-4 stimulation in muscle-derived primary culture cells by Northern blot analysis (A) and quantitation of the data of Northern blot analysis by Densitometry (B). G3PDH mRNA levels (*the bottoms of all lanes* are G3PDH) obtained by Northern blotting were used for normalization (A). The score on hour 0 (just after BMP stimulation) was used as a standard (B). The gene expression pattern of the molecules after stimulation of mBMP-4 (20%) was similar to that seen after stimulation of 100 ng/ml rhBMP-2

report using the pluripotent C2C12 cell line, and another study that revealed predominant expression of BMPR-1B in brain and not skeleton [20].

The induction of Noggin gene expression in cells of the osteoblastic lineage following exposure to rhBMP-2, and in fetal rat limb explants by BMP-7, has been reported [21,22]. In this study, Noggin gene expression was also confirmed in muscle-derived primary culture cells, an osteoblastic cell line (MC3T3-E1), and a nonosteoblastic, embryonic fibroblast-like cell line (NIH3T3) [16,23,24]. As Noggin is a representative antagonist of BMP action, the expression of

Noggin might act as a negative regulator of the BMP-induced cellular reactions, and consequently reduce the susceptibility of the cells to BMPs.

Three classes of Smads, termed receptor-activated Smads (R-Smads), common Smads (Co-Smads), and inhibitory Smads (I-Smads), have been identified in mammals. Smads1, 5, and 8 are R-Smads that primarily mediate BMP signaling from the receptors to the nucleus [16,25]. Therefore, the up-regulation of Smad-4, which is a representative BMP signaling Co-Smad, in a time- or dose-